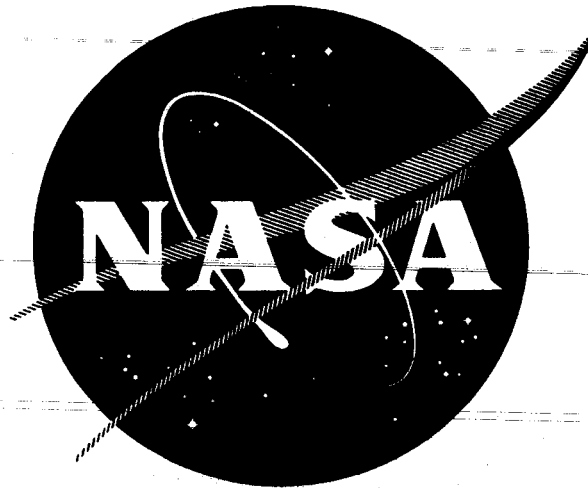


N65-19262

NASA CR-54,100

GA-5982



**DEVELOPMENT OF NEUTRON ACTIVATION ANALYSIS  
PROCEDURES FOR THE DETERMINATION  
OF OXYGEN IN POTASSIUM**

**FINAL REPORT**

Prepared for  
**National Aeronautics and Space Administration  
Lewis Research Center  
Under Contract NAS3-2537**

**GENERAL ATOMIC**

DIVISION OF

**GENERAL DYNAMICS**

**JOHN JAY HOPKINS LABORATORY FOR PURE AND APPLIED SCIENCE**

**P.O. BOX 608, SAN DIEGO 12, CALIFORNIA**

NASA CR-54,100

GA-5982

DEVELOPMENT OF NEUTRON ACTIVATION ANALYSIS  
PROCEDURES FOR THE DETERMINATION  
OF OXYGEN IN POTASSIUM

Final Report

(Period Ending December 15, 1964)

By

E. L. Steele

H. R. Lukens, Jr.

V. P. Guinn

Sponsored by

National Aeronautics and Space Administration  
Lewis Research Center

Technical Management

NASA-Lewis Research Center

Nuclear Power Technology Branch

R. A. Lindberg

GENERAL ATOMIC DIVISION

GENERAL DYNAMICS CORPORATION

John Jay Hopkins Laboratory for Pure and Applied Science

P. O. Box 608, San Diego, California

Contract: NAS3-2537

NOTICES

This report was prepared as an account of Government-sponsored work. Neither the United States nor the National Aeronautics and Space Administration (NASA), nor any person acting on behalf of NASA:

- A) Makes any warranty or representation, expressed or implied, with respect to the accuracy, completeness, or usefulness of the information contained in this report, or that the use of any information, apparatus, method, or process disclosed in this report may not infringe privately owned rights; or
- B) Assumes any liabilities with respect to the use of, or for damages resulting from the use of any information, apparatus, method or process disclosed in this report.

As used above, "person acting on behalf of NASA" includes any employee or contractor of NASA, or employee of such contractor, to the extent that such employee or contractor of NASA or employee of such contractor prepares, disseminates, or provides access to, any information pursuant to his employment or contract with NASA, or his employment with such contractor.

AVAILABILITY NOTICE

Qualified requestors may obtain copies of this report from:

National Aeronautics and Space Administration  
Office of Scientific and Technical Information  
Washington 25, D. C.  
Attn: AFSS-A

## TABLE OF CONTENTS

TITLE PAGE	
NOTICES . . . . .	ii
TABLE OF CONTENTS . . . . .	iii
LIST OF FIGURES . . . . .	v
LIST OF TABLES . . . . .	v
I. INTRODUCTION . . . . .	1
II. PRINCIPLES OF ACTIVATION ANALYSIS . . . . .	3
Thermal-Neutron Activation Analysis . . . . .	3
Fast-Neutron Activation Analysis . . . . .	4
III. TECHNIQUES OF ACTIVATION ANALYSIS . . . . .	6
IV. EQUIPMENT . . . . .	9
Neutron Sources . . . . .	9
250-kw TRIGA Mark I Nuclear Reactor . . . . .	9
150-kv Cockcroft-Walton Deuteron Accelerator . . . . .	9
Automatic Control System . . . . .	10
Transfer System . . . . .	10
Detection Systems . . . . .	13
Sodium Iodide System . . . . .	13
Cerenkov System . . . . .	16
Accelerator Facility . . . . .	18
Inert-Atmosphere Handling System . . . . .	18
V. DETERMINATION OF OXYGEN BY ACTIVATION WITH FAST NEUTRONS . . . . .	19
Discussion . . . . .	19
The $O^{16}(n, p)N^{16}$ Reaction . . . . .	19
Decay Scheme of $N^{16}$ . . . . .	19
Sensitivity . . . . .	19
Procedure . . . . .	20
Irradiation Time . . . . .	20
Counting Time . . . . .	20
Standard Calibration . . . . .	21
Data Reduction . . . . .	21
Reactor Irradiation . . . . .	21
Accelerator Irradiation . . . . .	27
Precision . . . . .	27
Accuracy . . . . .	29

Determination of Oxygen in NASA-Lewis Potassium	
Samples . . . . .	29
Sources of Error . . . . .	35
Interelement Effect, $F^{19}(n, \alpha)N^{16}$ . . . . .	35
Beta-Gamma Overlap . . . . .	35
Recoil Interference . . . . .	38
Beta-Gamma Attenuation . . . . .	39
Pulse Pileup . . . . .	39
Flux Gradient . . . . .	40
VI. SUMMARY AND CONCLUSIONS . . . . .	41
VII. FUTURE WORK . . . . .	44
VIII. REPORTABLE ITEMS OF NEW TECHNOLOGY DURING REPORT PERIOD . . . . .	45
REFERENCES . . . . .	46

## LIST OF FIGURES

1. Front panel of automatic control unit . . . . .	11
2. Wiring diagram of automatic control unit . . . . .	12
3. Schematic diagram of transfer system . . . . .	14
4. Radiation terminal end . . . . .	15
5. Decay scheme of $N^{16}$ . . . . .	17
6. Effect of 98 mr/hr $Cl^{38}$ level on $N^{16}$ spectrum, using Cerenkov counter . . . . .	26
7. Twin-crystal detection system . . . . .	28

## LIST OF TABLES

1. Photopeak specific activities in reactor irradiations . . . . .	23
2. $N^{16}$ CPM per gram of oxygen with Cerenkov counter after 0.25-minute irradiation in the TRIGA Mark I reactor . . . . .	24
3. Cerenkov counter background . . . . .	25
4. Oxygen determination in standards (reactor activation) . . . . .	25
5. Determination of oxygen in hydrogen-fired OFHC copper . . . . .	30
6. Determination of oxygen in high-purity metals . . . . .	31
7. Determination of oxygen in niobium-encapsulated potassium . . . . .	31
8. Comparison of activation analysis with vacuum fusion for oxygen determination in metals . . . . .	32
9. Oxygen content of possible capsule materials . . . . .	33
10. Determination of oxygen in NASA-Lewis potassium samples . . . . .	34
11. Determination of oxygen in potassium samples from NASA contractors . . . . .	36
12. Products of the fast-neutron irradiation of some common matrix and impurity elements . . . . .	37
13. Concentration of element required to give same count as 100 ppm oxygen . . . . .	38
14. Results of irradiation in presence of oxygen gas . . . . .	38
15. Beta-gamma attenuation . . . . .	39
16. Effect of sample rotation during neutron irradiation . . . . .	40

## I. INTRODUCTION

The increased utilization of potassium and other alkali metals in space-related research and development projects has created a demand for new analytical techniques in this area. Absolute control of certain impurities is essential for the high-performance tasks now in the planning stages. Oxygen, in particular, presents a problem because of its tremendous affinity for active metals. The important effects of oxygen concentration on the physical and chemical properties of the host matrix result in a need for a rapid and accurate method for determination of this element. A number of specialized methods have been reported for the determination of oxygen, (1-4) but only nuclear activation analysis(5) offers an almost completely general approach to the problem. A wide variety of nuclear reactions is available to the analyst for oxygen determination, e. g. ,  $O^{18}(p, n)F^{18}$ , (6)  $O^{16}(d, n)F^{17}$ , (7)  $O^{16}(t, n)F^{18}$ , (8)  $O^{16}(\gamma, n)O^{15}$ , (9)  $O^{18}(n, \gamma)O^{19}$ , (10)  $O^{17}(n, \alpha)C^{14}$ , (11) and  $O^{16}(n, p)N^{16}$ . (5, 12, 13)

For a number of reasons, it was felt by the present investigators that neutron-induced reactions offered the most effective approach for oxygen determination in alkali metals. Furthermore, it appeared that the neutron-proton reaction on  $O^{16}$  was the reaction best suited for the average analytical laboratory--from considerations of time required per analysis, equipment availability and cost, concentration sensitivity, and convenience. Therefore, a proposal entitled "Determination of Oxygen in Potassium" was submitted by General Atomic to the National Aeronautics and Space Administration. This proposal led to the present research contract.

The intent of this contract was to develop an activation analysis procedure for the determination of oxygen in potassium which incorporated the latest developments in the state of the art. To accomplish this objective, the experimental work, during the contract, was directed toward:

1. Investigation of fission-spectrum fast neutrons produced by the uranium-235 fission reaction (in a nuclear reactor) as a possible neutron source to induce the  $O^{16}(n, p)N^{16}$  reaction.
2. Investigation of small Cockcroft-Walton positive-ion accelerators as possible sources of 14-Mev neutron, produced by the deuterium-tritium reaction, to induce the  $O^{16}(n, p)N^{16}$  reaction.
3. Investigation of Cerenkov detection systems as a means of measuring the highly energetic beta particles emitted in the decay of  $N^{16}$ .

4. Investigation of sodium iodide detection systems, with modified electronic circuitry, as a means of measuring the 6.1- and 7.1-Mev gamma rays from the decay of the excited state of  $O^{16}$ .
5. Design and construction of an automated neutron-activation analysis system which would precisely control such variables as irradiation time, transfer time, and geometry conditions of the irradiation and detection procedures.
6. Design and construction of a pneumatic transfer system that would move samples from the neutron source to the detectors in less than one second.
7. Design and construction of special sample containers for alkali metals--containers capable of withstanding the impact experienced in a rapid transfer system.
8. Determination of the oxygen content of various materials which could serve as sample containers.
9. Investigation of various metal-cleaning techniques to reduce the container blank.
10. Determination of the lower limit of detection of the analytical method.
11. Determination of the precision of the analytical method.
12. Determination of the accuracy of the analytical method.

As a result of this program, an analytical method for the determination of oxygen in potassium has been developed that is exceptionally rapid, quite precise and accurate, and highly sensitive. The entire procedure, including irradiation, transferring, counting, and data reduction, requires less than two minutes per sample. Sample encapsulation and weighing together require an additional five minutes per sample. At the level of 30 micrograms of oxygen (30 ppm in a 1-gram sample) precision for a single irradiation is approximately  $\pm 30\%$  of the value. This precision value can be significantly improved by the averaging of repeat determinations. At the level of 100 micrograms of oxygen, the precision is  $\pm 10\%$  of the value (for a single determination). At still higher oxygen levels, the precision approaches  $\pm 1\%$  of the value. The sensitivity of the method (if defined as the level at which the signal is of the same size as the background) is 25 micrograms of oxygen. OFHC copper was found to be a suitable capsule material for routine determinations in the range of 25 to 500 micrograms of oxygen.



## II. PRINCIPLES OF ACTIVATION ANALYSIS

Nuclear activation analysis is a method for qualitatively and quantitatively determining elemental composition by means of nuclear transmutations. The method begins with the irradiation of samples for analysis with subatomic particles or high-energy electromagnetic radiation for the purpose of creating radioactive isotopes for subsequent measurement from elements present in the sample. Artificial isotopes formed in this manner are characteristic, in numbers and types, of the isotopic composition of the original sample and the irradiation conditions. Assuming a uniform and characteristic isotopic distribution in nature, a uniform radiation source, and a uniform measuring system, the only variable in radioisotope production for elemental analysis is concentration. In practice, the analyst seldom has a uniform radiation source. As a result, the total isotope production is a summation of all events possible within the perimeters of a given radiation environment.

### THERMAL-NEUTRON ACTIVATION ANALYSIS

This is the method most widely used in activation analysis work. It refers to a bombardment of samples with neutrons that are in thermal equilibrium with their environment. In practice this is room temperature, giving the neutrons an average energy of 0.025 electron volts (ev). With few exceptions, the type of induced nuclear reaction at this energy is the so-called neutron-gamma ( $n, \gamma$ ), or capture, reaction.

While the samples are being irradiated, two processes are occurring. New nuclei are constantly being formed at a rate equal to  $Nf\sigma$ , where  $N$  is the number of target nuclei of a given type present in the sample,  $f$  is the thermal-neutron flux to which the sample is exposed, expressed in units of neutrons per square centimeter per second, and  $\sigma$  is the capture cross section (capture probability), expressed in square centimeters per nucleus. Also, if these new nuclei are unstable (radioactive), they decay at a rate equal to  $N^*\lambda$ , where  $N^*$  is the number of product nuclei present at any time  $t$  and  $\lambda$  is the radioactive decay constant. The over-all net rate of formation of product nuclei is, therefore, the difference in the two rates:

$$dN^*/dt = Nf\sigma - N^*\lambda \quad (1)$$

This is a linear differential equation for which the solution is

$$N^* = Nf\sigma(1 - e^{-\lambda t})/\lambda \quad (2)$$

In practice, one is interested in the decay rate,  $\lambda N^*$ , rather than in  $N^*$ . Rearrangement of Eq. (2) gives this as

$$N^* \lambda = N f \sigma (1 - e^{-\lambda t}), \quad (3)$$

which is the activity in units of disintegration per second after an irradiation time  $t$ .

Of course,  $N$  is a function of the sample weight, the percent of the element present (% of el.), the abundance of the target nuclide in question (% ab.) among the stable nuclides of that element, the atomic weight of the element, and of Avogadro's number. Thus, the activity  $A$ , in dis/sec, is

$$\frac{\text{sample wt} \times \frac{\% \text{ of el.}}{100} \times \frac{\% \text{ ab.}}{100} \times (6.02 \times 10^{23}) \times f \sigma (1 - e^{-0.693t/T})}{\text{chemical atomic weight of element}}. \quad (4)$$

From Eq. (4), it is obvious that the activity produced by the  $(n, \gamma)$  reaction for a given sample depends on the neutron flux and the time of irradiation. Saturation (steady state) is reached when  $t \gg T$ , where  $T$  is the half-life of the product nuclide. In this case,  $(1 - e^{-\lambda t})$  approaches unity. Similarly, the activity is  $1/2 A_{\text{sat}}$  at  $t = T$ ,  $3/4 A_{\text{sat}}$  at  $t = 2T$ ,  $7/8 A_{\text{sat}}$  at  $t = 3T$ , and so on.

### FAST-NEUTRON ACTIVATION ANALYSIS

There is no universally accepted definition for analysis based on fast-neutron-induced reactions. In general, the term is applied to systems which produce radioactive products by the nuclear reaction  $X(n, b)Y$ , where  $n$  is an energetic neutron and  $b$  is a nuclear particle (not a gamma ray). This would include such reactions as the  $(n, p)$ ,  $(n, 2n)$ ,  $(n, \alpha)$ ,  $(n, d)$ ,  $(n, t)$ ,  $(n, n')$ , and  $(n, np)$  reactions. The thresholds for these particle-particle reactions, e. g., the energies required to induce the reactions, with few exceptions are in the range of millions of electron volts (Mev). The particular reaction that will dominate under a given set of conditions is a function of the nucleus involved and the energy associated with the incoming neutron. For example, the common isotope of oxygen ( $O^{16}$ ) does not interact with a fast neutron unless the neutron has a minimum energy of about 10 Mev, but when it does react, the probability is that it will absorb the neutron and promptly emit a proton within a period of about  $10^{-14}$  sec. The over-all result is that an energetic neutron ( $>10$  Mev) will produce a  $N^{16}$  nucleus when it reacts with  $O^{16}$ . The  $N^{16}$  isotope is radioactive ( $T = 7.35$  sec) and can be measured readily. The  $(n, \alpha)$  reaction on  $O^{16}$  produces only the stable (nonradioactive) isotope  $C^{13}$ . The  $(n, 2n)$  reaction on  $O^{16}$  requires

a neutron energy greater than 14 Mev. The common isotope of nitrogen ( $N^{14}$ ) is very unusual in that it will undergo the (n, p) reaction at a neutron energy of <1 ev to produce  $C^{14}$ . With neutrons of energy beyond about 10 Mev,  $N^{14}$  undergoes a (n, 2n) reaction to produce  $N^{13}$ . Carbon-14 is a very long-lived ( $T = 5700$  years) radioisotope, whereas  $N^{13}$  is quite short-lived ( $T = 10$  min). It is a simple task to measure  $N^{16}$  in the presence of  $N^{13}$ , and vice versa, because of the great differences in their half-lives and radiation energies.

It is possible to draw several conclusions from the vast amount of experimental data available concerning fast-neutron reactions. First, the (n, p) reactions generally require less energetic neutrons than do (n, 2n) reactions. The probability for the (n, 2n) reaction is generally very low, below about 10 Mev except for elements of high atomic number. The (n, 2n) reactions are all endoergic, mostly having thresholds in the range of 8 to 12 Mev. Second, the probability for (n,  $\alpha$ ), (n, d), and (n, t) reactions goes down with increasing atomic number (due to coulomb barrier effects). Third, the probability of fast-neutron reaction, i. e., the cross section of the reaction, is usually less than the probability of thermal-neutron capture.

A problem in calculating expected detection sensitivities for fast-neutron-induced reactions is the energy dependence of the reaction cross section. The reaction cross-section term varies with neutron energy, and at the present time it is difficult to predict the behavior quantitatively. In practice this is not a problem, because a known sample activated under the same experimental conditions permits a concentration calculation by a simple ratio method.

### III. TECHNIQUES OF ACTIVATION ANALYSIS

Activation analysis can be applied to the determination of almost every element of the periodic system down to levels in the microgram to submicrogram range. For a given problem, the method to be employed is a function of the matrix properties, trace elements, sensitivity requirements, costs, and the properties of the element in question. The selection of activation analysis as the appropriate technique to solve an analytical problem is usually based on its sensitivity, speed, economy, and convenience, or on the absence of other suitable methods. Sufficient qualitative and quantitative experimental data exist in most cases to enable one to select the most appropriate activation-analysis technique. In general, the following sequence of considerations is involved:

1. Selection of the optimum nuclear reaction.
2. Selection of a suitable irradiation facility.
3. Preparation of the sample for irradiation.
4. Determination of the irradiation time to be used.
5. Selection of a chemical separation scheme, if necessary.
6. Selection of a suitable postirradiation counting method.

The choice of nuclear reaction is usually based on the physical, chemical, and nuclear properties of the matrix and trace elements, and their activation products. These properties limit the instrumental sensitivity of a given nuclide and may dictate the necessity of chemical treatment after irradiation, before counting. Another factor is economics, since it is generally not feasible to have on hand equipment capable of furnishing a complete range of energies for all known projectiles. In the present treatment, of course, only neutrons are considered as the bombarding particles.

The selection of a neutron source is based on the energies and fluxes required. The nuclear reactor produces neutrons at very high fluxes, but the energies of these neutrons are predominantly very low. A 150-kv deuteron accelerator will produce 14-Mev neutrons, via the  $H^3(d, n)He^4$  reaction, but will not produce the high fluxes available in the reactor.

Sample preparation is usually not a problem. For neutron irradiation, the sample can be sealed in almost any container of convenient size. If a nondestructive method is employed, that is, one involving no chemical

separations, it is best to use a container material that does not become radioactive in the neutron field. This eliminates the necessity of changing containers before counting.

The optimum irradiation time is a function of the half-lives of the sample nuclei. The presence of an interfering isotope can frequently be tolerated by the proper choice of conditions. The determination of platinum and chlorine on an alumina catalyst support, for example, is hampered because of the intense  $\text{Al}^{28}$  activity produced ( $T = 2.3$  min). This problem is easily solved by irradiating the samples for an hour and letting the  $\text{Al}^{28}$  decay away before counting for the activated platinum (30-min  $\text{Pt}^{199}$ ) and chlorine (37-min  $\text{Cl}^{38}$ ).

Postirradiation chemical separations are employed when the presence of an interfering isotope cannot be sufficiently minimized by varying the irradiation time or counting method. In general, the methods employed are standard chemical reactions. The addition of a carrier, that is, a known amount of the same element in nonradioactive form as the radioisotope to be separated, to the irradiated samples allows the analyst to use nonquantitative separation procedures. All that is necessary is that the percentage yield be determined. Naturally, the higher chemical yields produce the most sensitive methods.

If an absolute assay method is employed, i. e., the concentration is calculated from the disintegration rate, the assay must be quantitative. The neutron flux and the reaction cross sections must also be known for this method. With a comparative procedure, where a known sample is irradiated simultaneously, and counted identically, the absolute values of flux, cross sections, and activity need not be known quantitatively. The latter method is the more widely used, since it is generally more accurate.

As shown in Eq. (4), elemental sensitivity to neutron techniques is mainly a function of isotopic abundance, reaction cross section, and neutron flux; radioisotope half-life and decay scheme are also important parameters. Of the four known neutron-induced reactions of the oxygen isotopes that result in the formation of a radioisotope, i. e.,  $\text{O}^{16}(\text{n}, \text{p})\text{N}^{16}$ ,  $\text{O}^{16}(\text{n}, 2\text{n})\text{O}^{15}$ ,  $\text{O}^{17}(\text{n}, \alpha)\text{C}^{14}$ ,  $\text{O}^{18}(\text{n}, \gamma)\text{O}^{19}$ , the neutron-proton reaction with  $\text{O}^{16}$  is definitely the most suitable for the determination of small amounts of oxygen in potassium (or in other materials). The  $\text{O}^{16}(\text{n}, 2\text{n})\text{O}^{15}$  reaction requires neutron energies in the range of 15+ Mev, which are produced in quantity only by large accelerators. The  $\text{O}^{17}(\text{n}, \alpha)\text{C}^{14}$  reaction requires impossibly long irradiation times owing to the 5700-year half-life of  $\text{C}^{14}$ . Also,  $\text{C}^{14}$  emits only soft beta particles -- no gamma rays. The  $\text{O}^{18}(\text{n}, \gamma)\text{O}^{19}$  reaction has a very small cross section, and the isotopic abundance of  $\text{O}^{18}$  is small (0.2%). The  $\text{O}^{16}(\text{n}, \text{p})\text{N}^{16}$  reaction readily produces a short-lived radioisotope ( $T = 7.35$  sec). This reaction only

requires neutrons of energies in a more readily accessible range, above about 10 Mev.

Neutrons in the 10- to 15-Mev range are available from both nuclear reactors and accelerators. In the case of reactors, the 10- to 15-Mev neutron flux is several orders of magnitude lower than the flux of very low-energy neutrons because of the primary fission neutron spectrum and the great degree of moderation required to sustain the fission process. Accelerators, on the other hand, can produce only fast neutrons, if desired-- neutrons with energies depending on the nature and energy of the projectile and on the target material. Small, inexpensive, low-voltage accelerators can produce these very energetic neutrons, but they are limited to the thermonuclear reaction  $\text{H}^3(\text{d}, \text{n})\text{He}^4 + 17.6 \text{ Mev}$ , of which 4/5 goes to the neutron produced, and 1/5 goes to the alpha particle.

## IV. EQUIPMENT

### NEUTRON SOURCES

#### 250-kw TRIGA Mark I Nuclear Reactor

The TRIGA Mark I reactor was used for all reactor experiments. At the 250-kw power level, this reactor produces a flux of  $4.3 \times 10^{12}$  thermal neutrons/cm<sup>2</sup>-sec in the pneumatic-tube position. In the same position, there are lower fluxes of high-energy neutrons:  $3.5 \times 10^{12}$  neutrons >0.01 Mev,  $7.5 \times 10^{11}$  neutrons >1.35 Mev,  $1.25 \times 10^{11}$  neutrons >3.7 Mev, and  $1.9 \times 10^{10}$  neutrons >6.1 Mev. The reactor can also be "pulsed" to about  $10^9$  watts for approximately 15 msec. During a pulse, the neutron flux exceeds  $10^{16}$  neutrons/cm<sup>2</sup>-sec.

The transit time from the sample irradiation position to the counting room is about 2 sec with the present pneumatic system. For reasons of safety, the sample containers are enclosed in a second rabbit. To reduce the thermal-neutron-induced reactions in some of the experiments, the outside rabbit is constructed with liners of boron, boron-10, or boron-10-cadmium.

#### 150-kv Cockcroft-Walton Deuteron Accelerator

Texas Nuclear Corporation Models 9500 and 9900 150-kv Cockcroft-Walton positive-ion machines were used as sources of 14-Mev neutrons. Each of these units consists of three separate sections: the accelerator with vacuum system, a 150,000-volt power supply, and a control console. The units are capable of producing neutrons with no further equipment necessary except a tritium target. Once the vacuum, deuterium gas pressure, extraction voltage, focus voltage, and solenoid current are adjusted to yield the desired level, a source of neutrons is available at the turn of a switch.

The reaction  $H^3(d, n)He^4$  is used to generate neutrons. In this highly exoergic reaction, the neutrons leave the target essentially isotropically with kinetic energies of approximately 14 Mev. For Model 9500, the maximum beam current ( $D^+$ -ions) is 1 milliampere. With a 150-kv accelerating potential and a tritium target of 3 to 5 curies per square inch, the neutron yield is about  $5 \times 10^{10}$  n/sec. The maximum neutron flux obtainable in the center of a 5-cm<sup>3</sup> sample is approximately  $5 \times 10^8$  n/cm<sup>2</sup>-sec. In the case of the larger machine, Model 9900, the maximum  $D^+$  beam current available is 2.5 milliamperes. The neutron yield, however, is  $2 \times 10^{11}$  n/sec. This is slightly more than 2.5 times the smaller model

and is explained on the basis of increased target area. With this machine, a 5-cm<sup>3</sup> sample can be exposed to an average flux of about  $2 \times 10^9$  n/cm<sup>2</sup>.sec.

### AUTOMATIC CONTROL SYSTEM

An automatic control mechanism was designed and installed to eliminate all manual operations in the analytical procedure. An operator inserts the sample, pushes the reset button, and dials the desired irradiation time. The sample and the monitor are automatically sent to the irradiation position, indicated by the panel lights. The system is started by energizing the clock, which turns on the accelerator. When the clock times out, the solenoid valve on the nitrogen jets opens, the exhaust valves are switched to OUT, the accelerator turns off, and the IRRADIATE TO ANALYZE timer is energized. Sample and monitor are transferred to their detector positions. When the IRRADIATE TO ANALYZE timer times out, the analyzers are turned on for a preset time. The counting data are displayed on two scalars. If there is any change in the sequence of events (logic-upset) a TILT light will turn on as a signal to disregard that determination.

Other features mounted on the control panel are:

1. Main POWER switch and light.
2. WATER (target cooling) light.
3. Accelerator BEAM light.
4. Automatic and manual ON and OFF switches.
5. READY light.
6. VALVE IN and OUT lights and switches.
7. BLOWER light and AUTO OFF-ON switch.

The entire assembly is in a standard 19-inch rack mount, 12 inches high and 15 inches deep. Figure 1 is a photograph of the front panel of this equipment and Fig. 2 is a wiring diagram of the electronic circuitry.

### TRANSFER SYSTEM

A dual sample transfer system was designed and built to accomplish the following objectives:

1. Move simultaneously a sample and standard from the neutron irradiation position to the detector position in one second or less.
2. Provide rotation for the sample and standard in the neutron beam to insure a more uniform irradiation.
3. Provide the operator with a visual indication of the sample location.



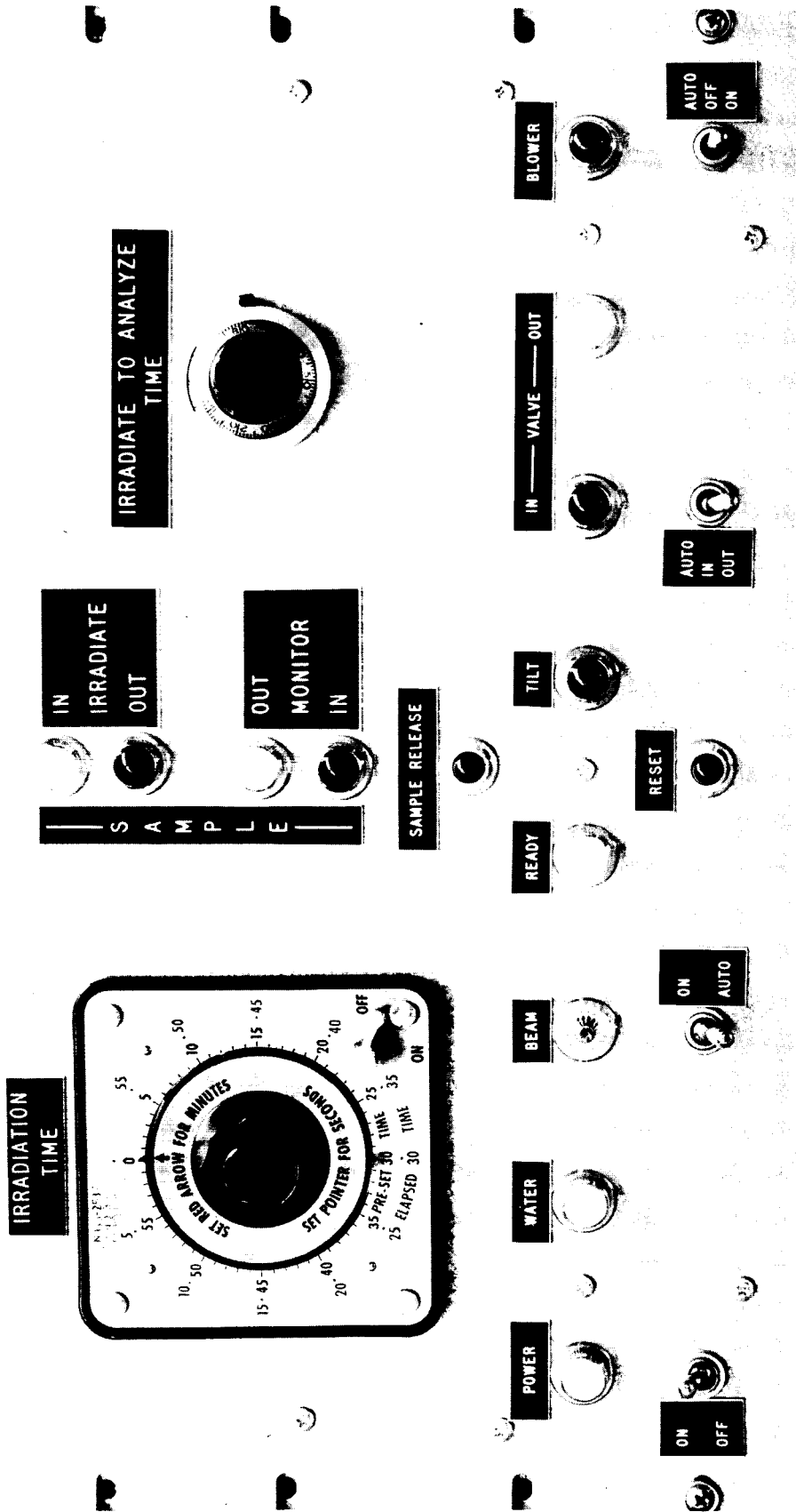


Fig. 1--Front panel of automatic control unit

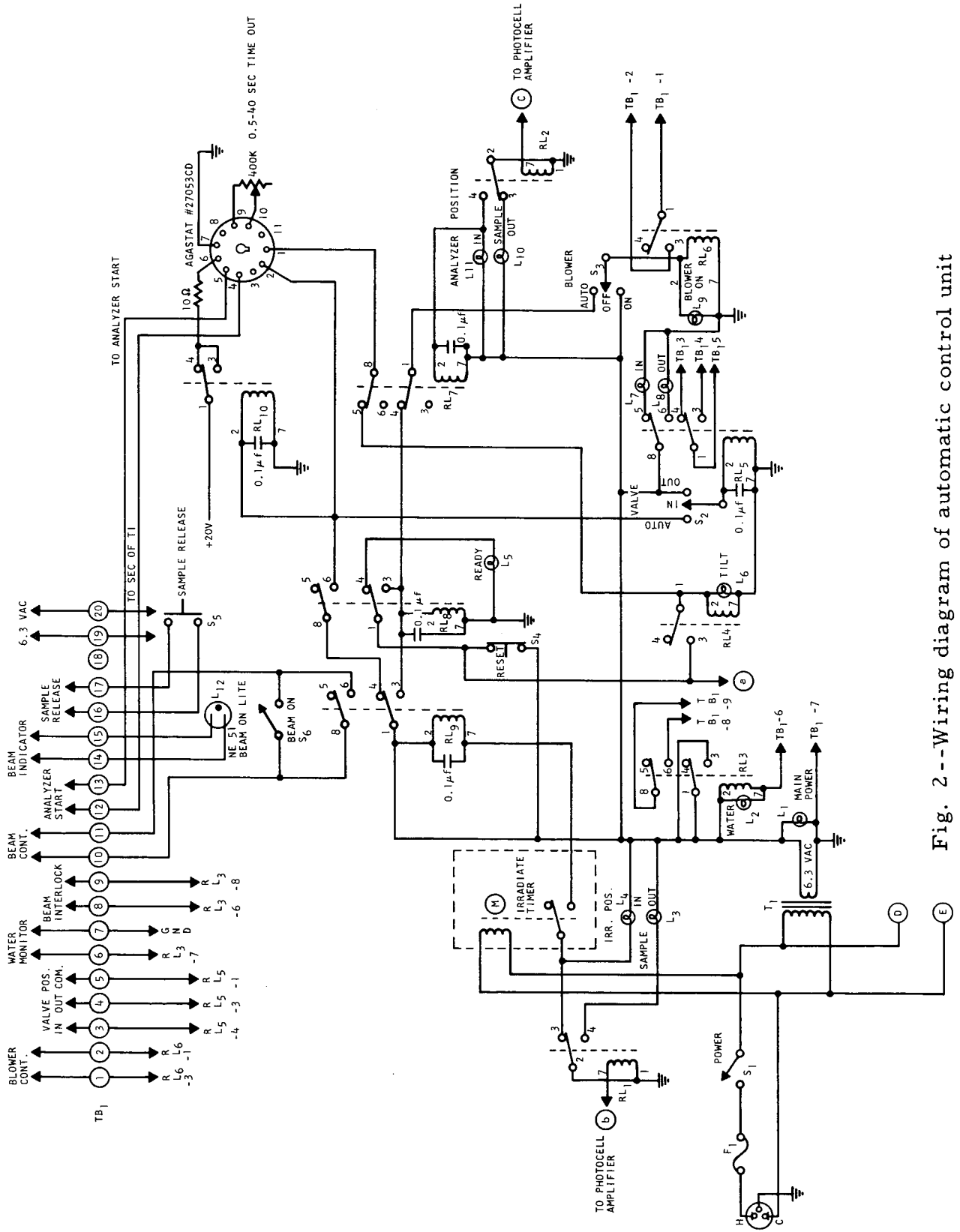


Fig. 2--Wiring diagram of automatic control unit

The sample travel time is a function of the gas velocity in the transfer tube and the time required for the force exerted by this gas to overcome the force of gravity. The basic features of this design are (1) the nitrogen jets that initially move the samples and (2) the large volume of nitrogen that carries the samples to the detector position. The nitrogen jets are powered by two cubic feet of dry nitrogen at a pressure of 50 to 80 psi. After each transfer, the nitrogen tank is refilled automatically from a nitrogen cylinder. A signal that operates the solenoids for the nitrogen also reverses the valves for the gas flow. A schematic diagram of the system is shown in Fig. 3.

Rotation of the sample and standard is provided by placing spindles between two blocks of metal at the irradiation position. Each spindle is attached to a gear in such a manner that a smaller gear in the center interlocks the whole mechanism with a single 94-rpm motor. This device is shown in Fig. 4.

A visual indication of sample position is provided by a set of photoelectric-cell-operated lights on the control console. These photocells are located at the irradiation position and at the counting position. By following the lights, an operator can tell whether or not a given sample has left or entered either end of the system. These lights are also used in the analytical procedure logic to prevent the system from starting when the samples are not in position.

## DETECTION SYSTEMS

### Sodium Iodide System

Interference in the detection of the 6.13- and 7.13-Mev gamma rays from  $N^{16}$  is not generally considered a problem. However, the fact that many elements have either a higher activation cross section than oxygen or a greater abundance in the sample, or both, often leads to a large amount of activity in addition to and relative to the  $N^{16}$  resulting from oxygen activation. The interfering activities may cause an inordinate amount of dead time in the measuring device, which seriously affects the counting statistics of the short-lived  $N^{16}$ . In addition, because of the relatively slow resolution time of the sodium iodide scintillation crystal ( $\sim 10^{-7}$  sec), it is possible for two or more gamma rays from a very radioactive source to be seen simultaneously and added prior to pulse-height analysis. Such pileup may raise the base of the  $N^{16}$  photopeak, which reduces the accuracy of the statistics of counting or obscures the photopeak altogether.

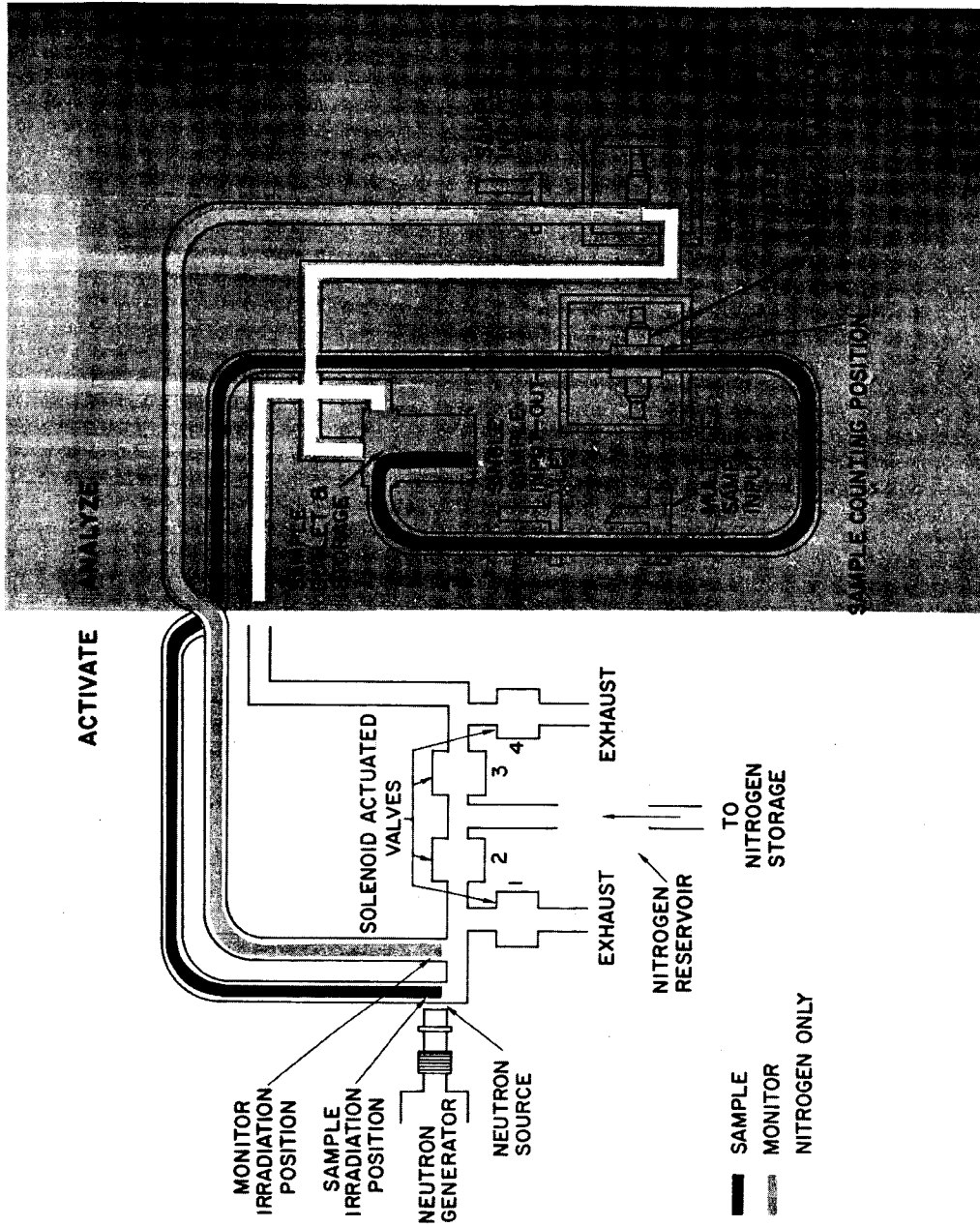


Fig. 3--Schematic diagram of transfer system

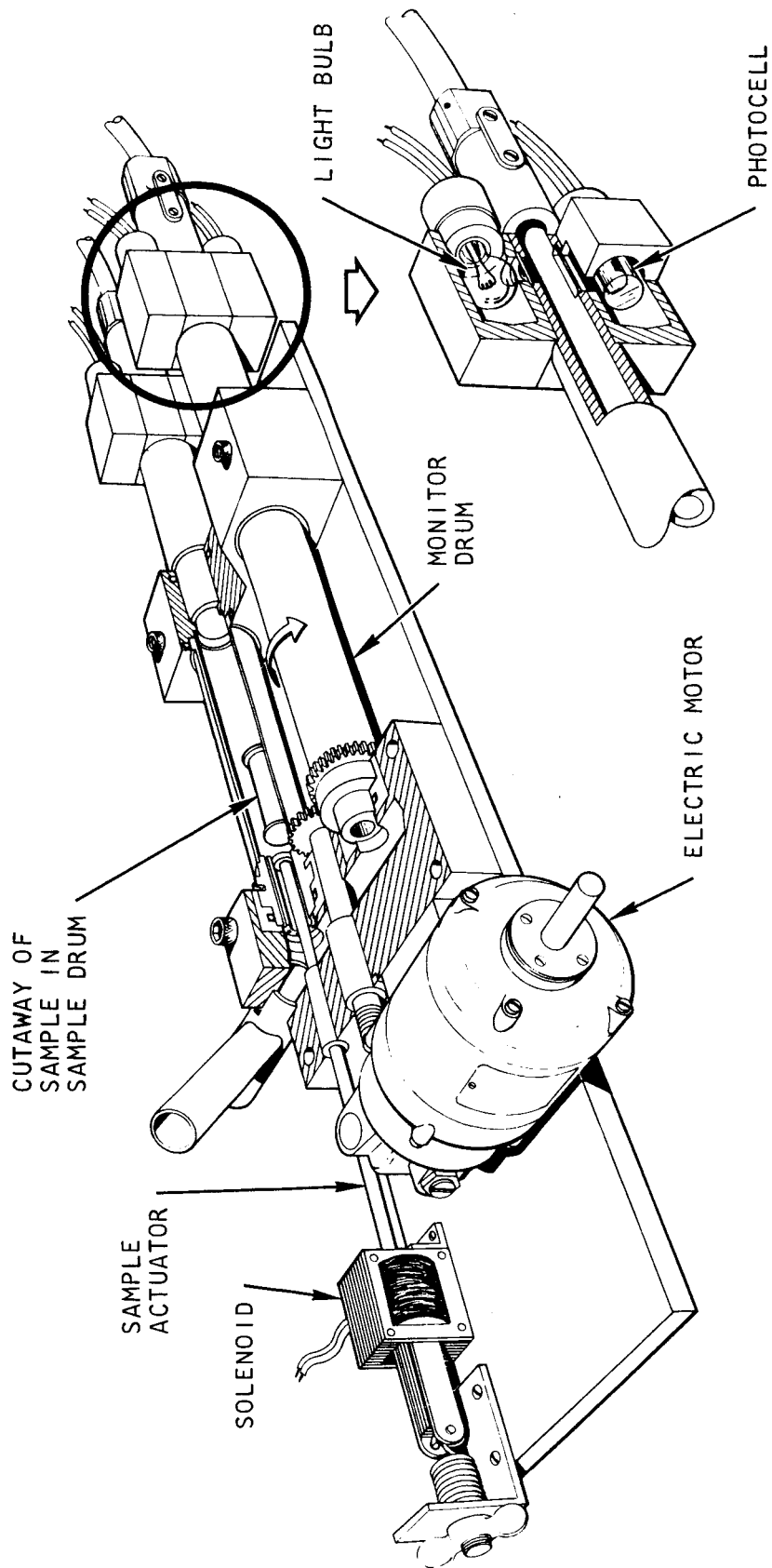


Fig. 4--Radiation terminal end

Two different techniques were used to minimize the potential pileup. First, a redesigned preamplifier that accepts the signal from the photomultiplier tube was tried. The new design has a resolution time of 1  $\mu$ sec, which is four times faster than the original device. The chance for pileup was reduced, then, by a factor of four. Electronic dead time was also reduced, making the entire system linear over a much larger concentration range.

### Cerenkov System

The second technique applied to this problem was the use of a Cerenkov detector. (1) Unlike the sodium iodide scintillation crystals previously used, this device measures the Cerenkov radiation from high-energy beta particles as a function of their energy. In general, when a charged particle traverses a path,  $l$ , in a medium, the number of photons radiated,  $N$ , along a short segment,  $d\ell$ , is given by

$$N = K \int_{\beta=\beta_{(\max)}}^{1/\eta} \left( 1 - \frac{1}{\beta^2 \eta^2} \right) d\ell ,$$

where  $\beta$  is the velocity of the particle relative to the velocity of light in a vacuum,  $\eta$  is the refractive index of the medium,  $1/\eta$  is the minimum velocity for the Cerenkov effect, and  $K$  is a combined constant that includes the fine structure constant and the radiation frequency range under consideration.

From the beta-particle energy sufficient to cause Cerenkov radiation in water (0.26 Mev), the photon output increases rapidly with beta energy up to about 2 Mev. Further increase in beta energy results in a smaller proportionate increase in light output, in accordance with the above equation. However, the number of beta particles of sufficient energy to cause a large Cerenkov radiation in water or Lucite increases markedly with increasing maximum energy of emission because of the energy-spectrum characteristics of beta emitters. Thus, the Cerenkov detector offers an advantage for measuring beta particles ( $10.4 \text{ Mev } E_{\max}$ ) from  $N^{16}$  in samples containing relatively large amounts of interference in the form of gamma rays or low-energy beta particles. In addition, the resolving time of the detector is of the order of only  $10^{-10}$  sec.

One disadvantage in counting only the high-energy beta particles from the  $N^{16}$  isotope is the relatively low abundance of these particles relative to the gamma rays. As seen from the decay scheme of  $N^{16}$  (see Fig. 5),  $\sim 75\%$  of the disintegrations proceed by emission of moderate-energy beta particles ( $E_{\max}$  values of 3.27 to 4.27 Mev) to two excited states of  $O^{16}$ . These excited states return to the ground state by gamma-ray

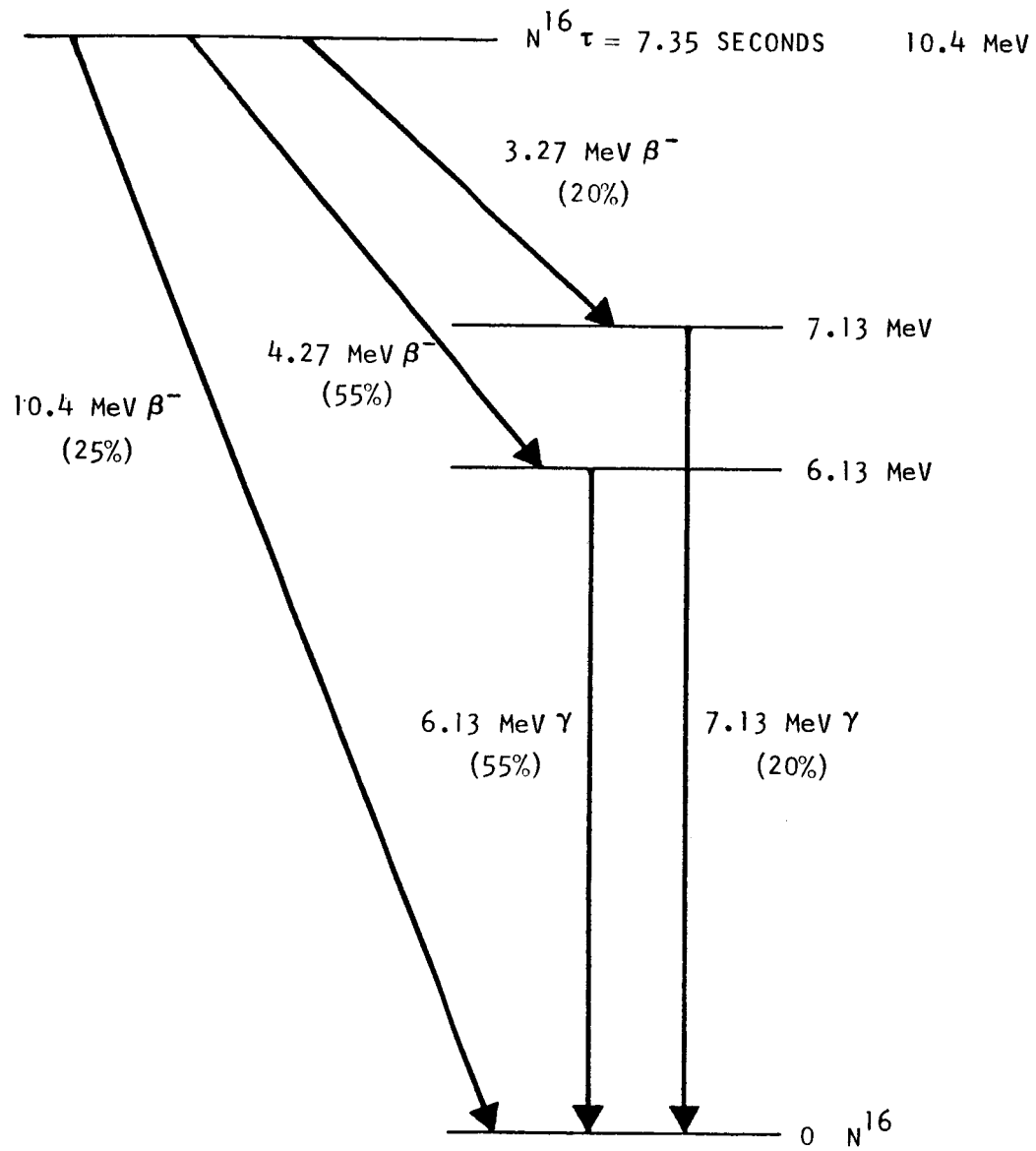


Fig. 5--Decay scheme of  $N^{16}$

emission. The remaining 25% of the decays go directly to the ground state of  $O^{16}$  by energetic beta emission (10.4 Mev  $E_{max}$ ). Thus, there are about three times as many moderate-energy gamma rays as there are highly energetic betas. The nature of beta emission, however, is such that the average beta energy is only about 1/3 of the  $E_{max}$ . It is the Cerenkov detector's efficiency for beta particles and insensitivity to gamma rays that makes it better for  $N^{16}$  detection than sodium iodide detectors. The fact that the Cerenkov detector is cheaper and more rugged is a further advantage.

### ACCELERATOR FACILITY

An underground location was selected for construction of the new accelerator facility. The design is a U-shape, with the two ends of the analytical system (irradiation and detection) only 14 feet apart. The polyethylene transfer-system tubing passes through a 6-foot arc, so that no direct line of sight exists between the target area and the detectors. The sample travel distance is 20 feet, and the transfer time for samples weighing less than 25 grams is approximately 0.5 seconds.

### INERT-ATMOSPHERE HANDLING SYSTEM

A new inert-atmosphere chamber has been installed for handling and encapsulating oxygen-sensitive samples. The unit consists of a hermetically sealed dry box combined with a highly efficient purification system that constantly maintains an inert atmosphere with less than 1 ppm moisture and oxygen. The purification system is basically a copper furnace followed by a soda-lime trap. Materials are inserted into the unit through a vacuum chamber, which is evacuated and back-flushed several times with purified argon. The box is equipped with induction heaters for outgassing, balances for weighing samples, and arc-welding torches for encapsulation. A MAGNEFORM\* head can be installed for magnetically sealing copper and aluminum capsules.

---

\* Registered in U. S. Patent Office.



## V. DETERMINATION OF OXYGEN BY ACTIVATION WITH FAST NEUTRONS

### DISCUSSION

#### The $O^{16}(n,p)N^{16}$ Reaction

The most widely used nuclear transmutation for the determination of oxygen by activation analysis is the  $O^{16}(n,p)N^{16}$  reaction, which was used in this investigation. The reaction is endoergic to the extent of 9.6 Mev. The requirement of conservation of momentum adds an additional 0.6 Mev, resulting in a reaction threshold energy of 10.2 Mev. Thus, for the reaction to be able to occur at all, the incident neutrons must have kinetic energies in excess of 10.2 Mev. Neutrons in this energy range are available from both nuclear reactors and small (150 kv) positive-ion Cockcroft-Walton accelerators.

#### Decay Scheme of $N^{16}$

The  $N^{16}$  product has a very short half-life (7.35 seconds) and decays by beta-particle emission to two of the excited states of  $O^{16}$  (~20% to one, ~55% to the other) or directly to the ground state of  $O^{16}$  (~25%). The excited states of oxygen decay by gamma-ray emission to the ground state in less than  $10^{-14}$  seconds. As a result of this decay pattern, approximately 75% of the transitions produce 3.27 or 4.27 Mev (max) beta particles, promptly followed by 6.13 or 7.13 Mev gamma-ray photons (55% 4.27 Mev  $\beta^- + 6.13$  Mev  $\gamma$ ; 20% 3.27 Mev  $\beta^- + 7.13$  Mev  $\gamma$ ). The other 25% of the transitions produce a 10.40 Mev (max) beta particle with no gamma rays. The unique character of the  $N^{16}$  isotope, i. e., its very high-energy beta particle and very high-energy gamma ray, makes it one of the easiest radioactive species to detect and measure. Either the beta or gamma radiation, or both, can be used for analytical purposes.

### SENSITIVITY

The sensitivity of the activation analysis method is generally expressed as the number of characteristic radiation counts detected per unit weight of the element in a given measurement time. The oxygen sensitivity, for example, could be expressed as the number of 6- to 7-Mev gamma-ray photoppeak counts obtained in 30 seconds of counting, per gram of oxygen. This implies

a particular irradiation configuration, neutron source, irradiation time, transfer time, and detection system. Sensitivity data can also be expressed as the minimum weight of the element in question that will produce a given number of characteristic counts. In either case, sensitivity values are a function of the analytical system and the procedure.

## PROCEDURE

Samples for analysis are packaged in polyethylene, stainless steel, or hydrogen-fired OFHC copper capsules and sealed. All handling, prior to the neutron irradiation, is done in a specially constructed inert-atmosphere box filled with purified argon. Capsules are sealed by electric welding techniques. Sample weights are obtained by weighing the capsules before and after loading. While still in the argon atmosphere, the capsules are placed in an air-tight container and transported to one of the analytical systems. For long storage, the permeability of polyethylene to oxygen gas can be a problem. Polypropylene is believed to be better in this respect.

### Irradiation Time

The irradiation time is selected on the basis of oxygen content and matrix effects. As mentioned previously, half of all the  $N^{16}$  activity the system will produce is obtained in 7.35 seconds. A 14.70-second irradiation will produce 75% of the maximum value. Irradiation times greater than 20 seconds can only add an additional 10% of the maximum but they can produce other problems by appreciable activation of the capsule and/or the matrix. For this reason, only in special cases are samples irradiated for longer than 20 seconds.

### Counting Time

At the end of the irradiation step, the sample and monitor are transferred to their respective detector positions and the radiation intensity of the characteristic gamma rays or beta particles of  $N^{16}$  is measured for 30 seconds. Since the decay of radionuclides is exponential and the half-life of  $N^{16}$  is short, it is important to move the samples from the neutron field to the detectors as rapidly as possible. Again, because of the rapid decay of  $N^{16}$ , counting times longer than 30 seconds for low oxygen levels produce few additional net counts. The counts for the unknown sample are normalized with the counts from the monitor and compared analytically with a known sample (also normalized) treated in an identical manner. Any irregularities in the neutron production, transfer times, or counting times are eliminated from the final calculation by this monitor technique.

### Standard Calibration

Analytical standards used as knowns in this comparator procedure consist of a specially prepared series of oxalic acid (AR grade) samples diluted with graphite. They are packaged in identical containers and are the same physical size and shape as the unknowns. A calibration curve of oxygen content versus activity allows a subtraction for blank oxygen by noting where the straight line crosses the activity axis at zero oxygen added. Other factors, such as gamma-ray attenuation, are discussed below. The oxalic acid-graphite standard samples are corrected for the small oxygen content (~0.3%) of the graphite.

### Data Reduction

In the procedure, then, the data for the oxygen determination are presented on one scaler and the neutron monitoring data are on a second scaler. The calculation to process an analytical number is as follows:

$$\frac{\text{Counts per mg O (known)}}{\text{Monitor counts}} = K$$

and

$$\frac{\text{Counts (unknown)} \times 100}{(K) (\text{Monitor counts}) (\text{Sample wt, in mg})} = \% \text{ O} .$$

### Reactor Irradiation

Samples for reactor irradiation were prepared in polyethylene vials having a 1-mm wall thickness, a 2.3-cm height, and a 1.0-cm inside diameter. The tops of the vials were heat-sealed with a soldering pencil after the samples were loaded. Irradiations were carried out with the sample vial contained in special rabbits to maintain a uniform sample position from one irradiation to another. Time in the neutron fields was varied from 15 seconds to 1 minute, as desired, except in the reactor-pulse experiments. At the completion of each irradiation, the time was recorded, and an electronic stop watch was used to measure the decay and counting times to the nearest one-hundredth of a second.

Several pulsing experiments were carried out to compare the generation of short-lived radionuclides by reactor pulsed irradiations with the results of steady-state irradiations. Radioactivity measurements were made by means of multichannel gamma-ray spectrometry. In all cases, a 0.5-inch polystyrene absorber was placed on the 3-inch by 3-inch NaI(Tl) detector to diminish the smearing of the gamma-ray spectra caused by beta particles from the sample.

The results of reactor irradiations of oxygen-containing samples are listed in Table 1. Also included are the results for aluminum, chromium, iron, vanadium, manganese, and potassium, obtained in a similar manner. The sensitivity of the oxygen method with this system varies from  $1.5 \times 10^6$  photopeak counts (6 to 7 Mev) per gram of oxygen for steady-state operation to  $2.1 \times 10^7$  photopeak counts (6 to 7 Mev) per gram of oxygen for pulsed operation. These data represent the ideal case where the matrix is not activated. Encapsulation in any of the standard containers made of copper, stainless steel, etc., however, produces so much activity that the electronic devices are not able to sort the pulses from the detectors.

In order to measure small amounts of  $N^{16}$  in the presence of large amounts of other activity, a Cerenkov detector was examined because of previous successes with this system at General Atomic. In those experiments a flat-bottomed glass vessel 3 inches in diameter and 2-1/2 inches high was filled with water, and a glass cover plate was cemented to the top. The device was placed on a 3-inch-diameter DuMont multiplier phototube. The assembly was held together and made light-tight with black tape. It was not shielded. Output from this detector was analyzed with a multichannel analyzer. Samples were sealed in polyethylene vials and activated in the TRIGA Mark I reactor.

The Cerenkov detector was investigated with respect to its response, at several phototube voltages and amplifier gains, to the beta radiations of  $N^{16}$  and  $Cl^{38}$ . The same radionuclides were also examined with a standard NaI(Tl) detector for comparison.

The sensitivity of detection of  $N^{16}$ , from the reaction  $O^{16}(n,p)N^{16}$ , varied with counting conditions as shown in Table 2. Activities shown in the table are corrected to counts per minute (CPM) per gram of oxygen at the end of the irradiation. Data are shown for certain groups of channels as well as for the total activity in all but the lowest four channels. The detector has the background characteristic shown in Table 3.

Two sets of three oxygen standards each were run in duplicate and the specific  $N^{16}$  activity was compared with that of the water standard. The results are shown in Table 4.

The spectra of  $Cl^{38}$  and  $N^{16}$  obtained with the Cerenkov detector are shown in Fig. 6. Three spectra are shown: one from 49.5 mg of chlorine as the ammonium salt; one from 48.5 mg of chlorine as  $NH_4Cl$  in 0.964 g of water; and one from 1.0732 g of water. The  $Cl^{38}$  activity level 3 minutes after irradiation was 98 mr/hr at 1 cm. The spectrum from  $Cl^{38}$  terminates at channel 34. Counts in channels  $\geq 35$  from the  $Cl-H_2O$  sample were taken to be due to  $N^{16}$  activity produced during irradiation via the  $O^{16}(n,p)N^{16}$  reaction. Calculation of the activity in channels  $\geq 35$  from both  $H_2O$  and

Table 1

## PHOTOPEAK SPECIFIC ACTIVITIES IN REACTOR IRRADIATIONS

Element	Irradiation Time (min)	Shield	Product Isotope	Photopeak Counts Per Gram
Oxygen	0.25	None	N <sup>16</sup>	1.5×10 <sup>6</sup>
	0.25	Boron	N <sup>16</sup>	1.5×10 <sup>6</sup>
	Pulse	None	N <sup>16</sup>	2.1×10 <sup>7</sup>
	0.25	Boron	O <sup>15</sup>	2.0×10 <sup>3</sup>
	0.25	None	O <sup>19</sup>	2.8×10 <sup>4</sup>
Aluminum	1.0	None	Al <sup>28</sup>	5.9×10 <sup>9</sup>
	1.0	B-Cd	Al <sup>28</sup>	1.1×10 <sup>8</sup>
	1.0	B-Cd	Mg <sup>27</sup> (0.84 Mev)	1.6×10 <sup>7</sup>
	1.0	B-Cd	Mg <sup>27</sup> (1.02 Mev)	5.1×10 <sup>6</sup>
	1.0	B-Cd	Na <sup>24</sup> (1.37 Mev)	6.5×10 <sup>4</sup>
	1.0	B-Cd	Na <sup>24</sup> (2.75 Mev)	1.7×10 <sup>4</sup>
Chromium	0.25	B <sup>10</sup> -Cd	V <sup>52</sup>	5.0×10 <sup>5</sup>
Iron	1.0	None	Fe <sup>59</sup>	1.7×10 <sup>3</sup>
	1.0	B-Cd	Fe <sup>59</sup>	9.9×10 <sup>1</sup>
	1.0	B-Cd	Mn <sup>54</sup>	2.7×10 <sup>2</sup>
	1.0	B-Cd	Mn <sup>56</sup>	2.9×10 <sup>5</sup>
Vanadium	0.25	None	V <sup>52</sup>	6.0×10 <sup>9</sup>
	0.25	B <sup>10</sup> -Cd	V <sup>52</sup>	1.5×10 <sup>8</sup>
Manganese	1.0	None	Mn <sup>56</sup>	6.1×10 <sup>9</sup>
	1.0	B-Cd	Mn <sup>56</sup>	2.2×10 <sup>8</sup>
Potassium	1.0	None	K <sup>42</sup>	1.2×10 <sup>6</sup>
	1.0	B-Cd	K <sup>42</sup>	4.6×10 <sup>4</sup>

Table 2  
 $N^{16}$  CPM<sup>a</sup> PER GRAM OF OXYGEN WITH CERENKOV COUNTER AFTER 0.25-MINUTE  
 IRRADIATION IN THE TRIGA MARK I REACTOR

Multiplier Phototube Voltage (v)	Amplifier Gain	Absorber	CPM per Gram of Oxygen				Total Specific Activity
			Channels 5-9	Channels 10-19	Channels 20-29	Channels >29	
900	1/4		$8.0 \times 10^5$	$1.3 \times 10^4$	$3.0 \times 10^3$	$2.3 \times 10^3$	$8.2 \times 10^5$
900	1		$3.0 \times 10^6$	$8.6 \times 10^5$	$8.1 \times 10^5$	$1.5 \times 10^5$	$4.8 \times 10^6$
900	1	Polyethylene, 1/2 in.	$1.07 \times 10^6$	$6.9 \times 10^5$	$2.5 \times 10^5$	$3.8 \times 10^4$	$2.1 \times 10^6$
900	1	Aluminum, 3/4 in.	$4.5 \times 10^5$	$3.6 \times 10^5$	$1.9 \times 10^5$	$2.7 \times 10^4$	$1.0 \times 10^6$
1100	1/4		$1.9 \times 10^7$	$3.0 \times 10^6$	$1.4 \times 10^6$	$7.6 \times 10^5$	$2.4 \times 10^7$
1100	1/2		$6.2 \times 10^7$	$2.0 \times 10^7$	$2.6 \times 10^6$	$3.2 \times 10^6$	$8.8 \times 10^7$

<sup>a</sup> CPM = counts per minute.

Table 3  
CERENKOV COUNTER BACKGROUND

Phototube Voltage (v)	Amplifier Gain	Channel Groups (CPM)				Total CPM
		5-9	10-19	20-29	>29	
900	1/4	36	32	0	0	68
900	1	5,156	92	8	4	5,260
1,100	1/4	50,080	2,568	20	4	52,672

Table 4  
OXYGEN DETERMINATION IN STANDARDS  
(REACTOR ACTIVATION)

Standard Sample <sup>a</sup>	Multiplier Phototube Voltage (v)	Amplifier Gain	Average <sup>d</sup> Oxygen (wt-%)	Actual Oxygen (wt-%)
Graphite-1 <sup>b</sup>	900	1	2.42 ± 0.07	2.54
Graphite-2	900	1	1.03 ± 0.03	1.06
Graphite-3	900	1	0.28 ± 0.02	0.29
Mineral oil-1 <sup>c</sup>	1100	1/4	0.125 ± 0.010	0.16
Mineral oil-2	1100	1/4	0.652 ± 0.012	0.664
Mineral oil-3	1100	1/4	1.130 ± 0.040	1.14

<sup>a</sup>All samples were sealed in polyethylene.

<sup>b</sup>Standardized with NaI detectors.

<sup>c</sup>Oxygen added as oxalic acid.

<sup>d</sup>By comparison of sample N<sup>16</sup> activity with the N<sup>16</sup> activity generated in water.

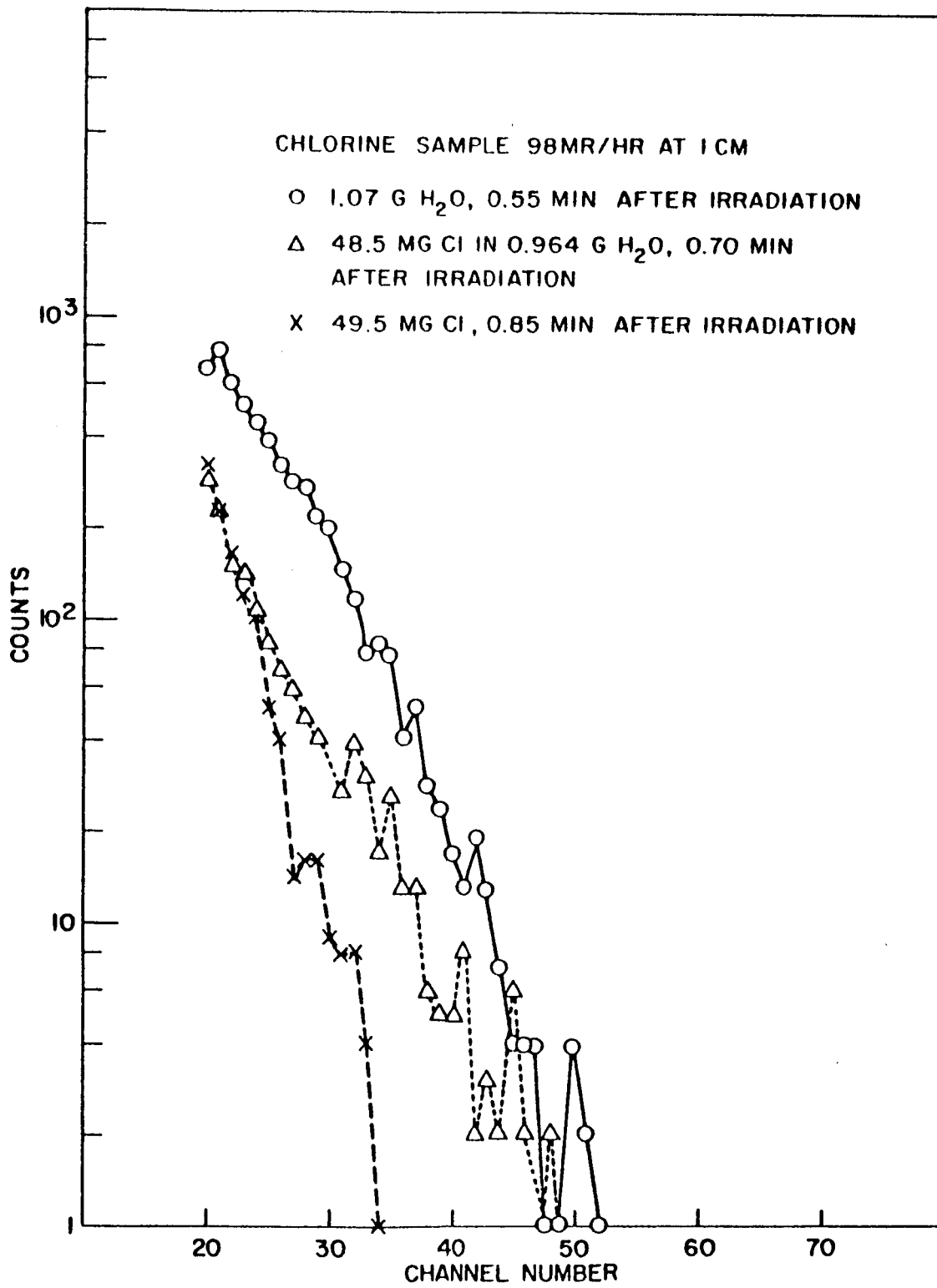


Fig. 6--Effect of 98 mr/hr Cl<sup>38</sup> level on N<sup>16</sup> spectrum,  
 using Cerenkov counter



H<sub>2</sub>O-C1 samples showed a sensitivity of  $6.30 \times 10^4$  cpm/g and  $6.15 \times 10^4$  cpm/g of oxygen, respectively.

Examination of the H<sub>2</sub>O-C1 sample was also attempted with a 3-inch by 3-inch NaI(Tl) detector using the same irradiation conditions. Pileup in the detector rendered it useless for this analysis.

For the current problem, that of oxygen in potassium, a Lucite cylinder was fitted with two 3-inch multiplier phototubes. A hole was drilled in the center to accommodate the transfer tube. The concept of two phototubes allows the utilization of coincidence electronic circuitry, which eliminates almost all electronic noise. Although the investigation of this detection system is still in the preliminary stages, sensitivities of better than 500 counts per milligram of oxygen have already been obtained, even in a gamma-ray background of 50 mr/hr.

### Accelerator Irradiation

Samples for accelerator irradiation were packaged in polyethylene, stainless steel, or OFHC copper capsules, as described above. They were transported to the accelerator system in an inert atmosphere and placed in the nitrogen-filled multiple-inlet device. This device is a part of the automated system that selects one sample at a time and places it in the transfer tube. Nitrogen gas was used to move the sample and monitor to the irradiation positions, and the procedure was started with a single switch. The sample and monitor were irradiated with 14-Mev neutrons for 20 seconds. They were then returned to their respective detectors (see Fig. 7) and the gamma rays greater in energy than 4 Mev were counted for 30 seconds with two 3-inch by 3-inch NaI(Tl) detectors and two single-channel pulse-height analyzers. At full beam power (2.5-ma beam current and 150-kv accelerating potential) the sensitivity for oxygen was found to be  $1.96 \times 10^6$  counts per gram of oxygen. The lower limit of detection of the method is taken as the point where the signal from the oxygen is equal to the background level in the detector (cosmic rays, etc.). In the present facility, the background for both detectors is approximately 50 counts per 30 seconds. This corresponds to a lower limit of oxygen detection of 25 micrograms.

### PRECISION

The limiting factor in the precision of the method is that resulting from the decay statistics. The theoretical precision obtainable, then, at the defined lower limit of 25  $\mu$ g of oxygen would be:

$$\begin{aligned}\sigma &= (\text{signal and background} + \text{background})^{1/2} \\ &= (100 \text{ counts} + 50 \text{ counts})^{1/2} \\ &= \pm 12 \text{ counts (or } \pm 6 \mu\text{g)}.\end{aligned}$$

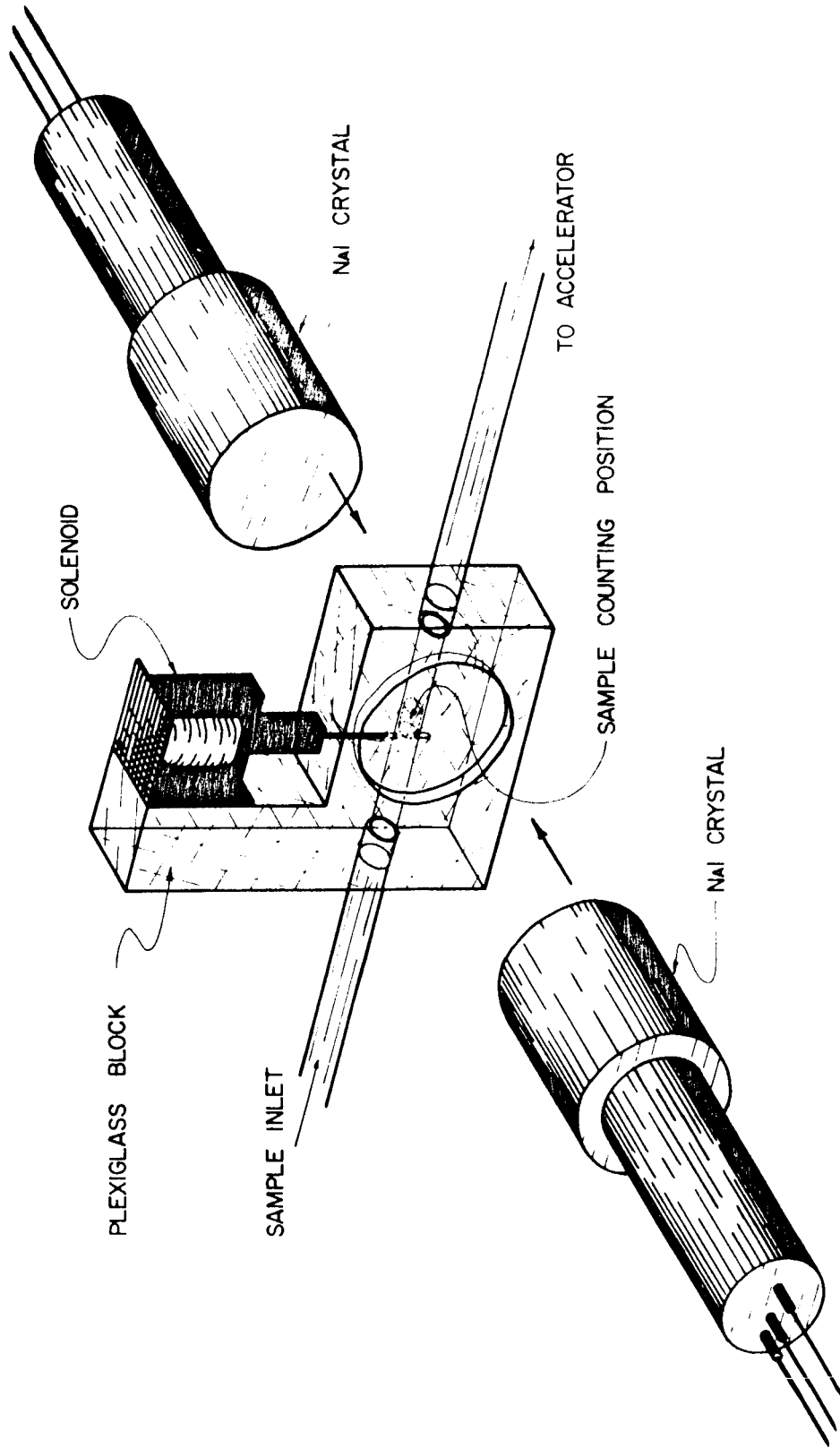


Fig. 7--Twin-crystal detection system

The lower limit is thus really  $25 \pm 6 \mu\text{g}$ . The sample examined that was closest to this lower limit was the OFHC copper used for the containers for the NASA potassium samples. These capsules weighed slightly over 18 grams and contained approximately 2 ppm oxygen. An average of 4 determinations gave an analytical value of  $35 \mu\text{g}$  per capsule, with an uncertainty of  $\pm 9 \mu\text{g}$ . Table 5 contains the data obtained from this experiment. At higher levels of oxygen, the percentage of uncertainty is much less. In the case of some specially prepared samples of tungsten and molybdenum, for example, the oxygen concentration was the same as in the OFHC copper, but the samples were much larger. These data are listed in Table 6.

Analytical precision, in the case of encapsulated samples, is also affected by the container-blank determination. A typical case emphasizing this problem was the cross-check sample of niobium-encapsulated potassium, undertaken jointly with the Oak Ridge National Laboratory (ORNL). This particular experiment was run in order to check the method with a second activation analysis laboratory. Two potassium samples and a niobium blank were prepared at ORNL. Since the inside diameter of the transfer system at ORNL is smaller than that at General Atomic, it was necessary to place the capsules inside polyethylene vials to transfer them. As a result, there were two blank corrections for each determination. The values found for K-1 and K-2 were  $0.15 \pm 0.1$  mg oxygen and  $2.87 \pm 0.13$  mg oxygen, respectively. These data are listed in Table 7. The sample weights were not available (but were about one gram), so ppm values are not listed in the table.

## ACCURACY

The accuracy of the neutron activation analysis method for the determination of oxygen was checked by analyzing a series of materials which were also analyzed by the more established vacuum-fusion method. As shown in Table 8, the comparison is quite good, indicating that the accuracy of the nuclear procedure is at least as good as that of the vacuum-fusion method. This same comparison has been made by a number of laboratories with similar results.

## DETERMINATION OF OXYGEN IN NASA-LEWIS POTASSIUM SAMPLES

Due to the large amount of activity generated in the various capsule materials in the reactor (see Table 1), even when they are shielded by  $\text{B}^{10}$  and/or cadmium, it was soon decided that the best neutron source for the determination of oxygen in potassium was the Cockcroft-Walton accelerator. Also, the sensitivity of the dual NaI(Tl) detector system was better by a

Table 5  
 DETERMINATION OF OXYGEN IN HYDROGEN-FIRED OFHC COPPER

Standardization Sample	Counts Std Sample	Monitor Counts	Counts per Monitor Count	Average Counts per Monitor Count	Counts per mg O per Monitor Count
28.3 mg O std	37,424	25,866	1.447	1.438 ( $\pm 0.9\%$ )	0.0508
	36,872	25,611	1.440		
	37,003	25,928	1.427		

Determination Sample	Weight (g)	Counts	Monitor Counts	Counts per Monitor Count	Oxygen	
					In ppm	In mg
Copper capsule	18.4378	53	25,156	0.0021	2.2	0.041
Copper capsule	18.4378	36	25,225	0.0014	1.5	0.028
Copper capsule	18.4378	40	24,998	0.0016	1.7	0.031
Copper capsule	18.4378	51	25,010	0.0020	2.1	0.039
						0.035 $\pm$ 0.009 avg

Table 6

## DETERMINATION OF OXYGEN IN HIGH-PURITY METALS

Sample	Weight (g)	Determination (ppm)			
		1st	2nd	3rd	Average
Tungsten-1	181.1	2.1	1.8	1.9	1.9±0.2
Tungsten-2	178.5	1.9	2.0	---	2.0±0.2
Tungsten-3	177.5	1.2	1.5	---	1.4±0.3
Molybdenum-1	94.4	6.9	6.9	---	6.9
Molybdenum-2	94.3	6.5	7.9	---	7.2±1.1
Molybdenum-3	94.1	5.9	7.1	---	6.5±0.9
Molybdenum-4	93.5	6.0	6.4	---	6.2±0.3

Table 7

DETERMINATION OF OXYGEN IN NIOBIUM-ENCAPSULATED POTASSIUM<sup>a</sup>

Sample	O Determination (mg)			
	1st	2nd	3rd	Average
Nb capsule + polyvial 1	2.10	2.19	2.14	2.14±0.05
Polyvial 1	1.72	1.61	1.68	1.67±0.07
Nb capsule	---	---	---	0.47±0.09
Nb capsule + K-1 + polyvial 2	2.14	2.12	2.10	2.12±0.02
Polyvial 2	1.45	1.54	1.50	1.50±0.05
Nb capsule + K-1	---	---	---	0.62±0.05
Nb capsule + K-2 + polyvial 3	5.07	5.20	5.12	5.13±0.08
Polyvial 3	1.72	1.81	1.83	1.79±0.07
Nb capsule + K-2	---	---	---	3.34±0.10

## Comparison of Results (in mg)

	General Atomic	ORNL
Oxygen in K-1 (0.69 g)	0.15±0.10 <sup>b</sup>	0.16 <sup>d</sup>
Oxygen in K-2 (0.75 g)	2.87±0.13 <sup>c</sup>	2.51 <sup>e</sup>
Oxygen in Nb capsule	0.47±0.09	0.45

<sup>a</sup>The experimental conditions were as follows: irradiation, 10 sec; counting, 30 sec; sensitivity, ~200 counts/mg oxygen; neutron flux,  $\sim 2 \times 10^8$  n/cm<sup>2</sup>-sec.

<sup>b</sup>Conc. of 217 ppm.

<sup>d</sup>Conc. of 232 ppm.

<sup>c</sup>Conc. of 3826 ppm.

<sup>e</sup>Conc. of 3346 ppm.

factor of 4 than the present Cerenkov detector system. Consequently, the NaI(Tl) system was used for all determinations involving potassium samples.

Table 8  
COMPARISON OF ACTIVATION ANALYSIS WITH VACUUM  
FUSION FOR OXYGEN DETERMINATION IN METALS

Sample	% Oxygen by Vacuum Fusion <sup>a</sup>	% Oxygen by Activation Analysis <sup>b</sup>
Titanium forgings		
No. 1	0.557	0.57
No. 2	0.082	0.088
Zircaloy		
No. 1	0.0911	0.087
No. 2	0.0752	0.079
Ferro-Al alloy	0.002	0.005
Deoxidized copper		
No. 1	0.007	0.010
No. 2	0.014	0.011
Stainless steel		
No. 1	0.003	0.005
No. 2	0.002	0.002
Nickel		
No. 1	0.137	0.14
No. 2	0.021	0.020
No. 3	0.005	0.004
Tantalum		
No. 1	0.11	0.11
No. 2	0.058	0.075

<sup>a</sup> Vacuum fusion data obtained by Kobe Steel Works, Ltd.

<sup>b</sup> Activation analysis data obtained by I. Fujii, *et al.* (14)

A number of metals were examined as possible containers, and a number of techniques were used, in an attempt to lower the blank values. The results of this study are listed in Table 9. The low-oxygen steel was unfortunately not available in quantities suitable for capsule construction. The copper containers sent to NASA-Lewis for potassium encapsulation

(2 ppm oxygen) were highly polished, vacuum-outgassed, and hydrogen-fired. Except for a research sample of tungsten, this was the best capsule material found. Polyolefins were examined but found to be unacceptable for potassium containers.

Table 9

## OXYGEN CONTENT OF POSSIBLE CAPSULE MATERIALS

Sample	Weight (g)	Sample Treatment	Oxygen Content	
			mg	ppm
OFHC copper	23.65	None	2.85	120
OFHC copper	22.43	Hydrogen furnace	0.206	9.2
OFHC copper	20.20	SiC sanding	0.667	33
OFHC copper	20.83	Filing	1.23	61
Brass	38.52	Vacuum furnace	3.51	91
Steel	43.30	Vacuum furnace	3.16	73
Molybdenum	15.18	Vacuum furnace	2.21	145
Molybdenum	14.95	Vacuum furnace	1.82	122
Niobium	5.18	Vacuum furnace	0.50	96
Niobium	5.21	Vacuum furnace	0.49	94
Steel	34.81	Zone refined	0.275	8
Steel	34.81	Zone refined	0.335	4
Steel	34.81	Zone refined	0.222	6

Prior to filling, the copper capsules were recleaned at NASA-Lewis, dried in acetone, and heated for one hour at 600°F in a hydrogen atmosphere. Approximately one gram of potassium was placed in each container, and the caps were welded in place at a pressure of  $10^{-5}$  torr. During the filling operation, several of the welded capsules leaked and were therefore discarded. The other capsules in the chamber tarnished, due to the potassium vapor, but were recleaned prior to analysis.

Each of the NASA-Lewis samples was irradiated for 20 seconds in a 14-Mev neutron flux of  $10^9$  n/cm<sup>2</sup>-sec. A counting time of 30 seconds was used for all samples, monitors, and standards. Three separate determinations were made on each sample, and these data are listed in Table 10. Also included in Table 10 are the results obtained at NASA-Lewis using the mercury amalgamation method. The relatively large uncertainty is due to the blank correction. In this case it was a copper capsule treated in the same manner as the samples.

Table 10

## DETERMINATION OF OXYGEN IN NASA-LEWIS POTASSIUM SAMPLES

Sample	Weight (g)	Mg Oxygen						Act. Anal. Results	Hg Amal. Results
		1st	2nd	3rd	Average	Blank	Net		
NASA Cu-1	1.0480	0.064	0.068	0.067	0.067±0.002	0.035±0.009	0.032±0.009	31±9 ppm	11 ppm
NASA Cu-2	1.0488	0.058	0.071	0.064	0.064±0.008	0.035±0.009	0.029±0.012	28±11 ppm	11 ppm
NASA Cu-4	1.1056	0.242	0.251	0.262	0.252±0.012	0.035±0.009	0.217±0.015	196±11 ppm	90 ppm
NASA Cu-7	1.0648	0.061	0.060	0.060	0.060±0.001	0.035±0.009	0.025±0.009	23±8 ppm	25 ppm
NASA Cu-8	0.7623	0.211	0.217	0.220	0.216±0.005	0.035±0.009	0.181±0.010	237±13 ppm	---
NASA Cu-9	1.0732	0.245	0.234	0.238	0.239±0.007	0.035±0.009	0.204±0.011	190±10 ppm	---
NASA Cu-10	1.3549	0.172	0.191	0.186	0.183±0.011	0.035±0.009	0.148±0.013	109±10 ppm	---
NASA Ta-2	1.1269	---	0.103	0.107	0.105±0.004	0.066±0.009	0.037±0.010	35±9 ppm	11 ppm
NASA Ta-3	1.0372	0.125	0.134	0.132	0.130±0.005	0.066±0.009	0.064±0.010	64±10 ppm	90 ppm
NASA Mo-2	0.8485	0.533	0.495	---	0.514±0.023	0.354±0.003	0.160±0.023	189±27 ppm	25 ppm



As part of this investigation, several potassium samples from two other laboratories were also examined for oxygen. In each case, OFHC copper tubing was supplied by General Atomic. The potassium was encapsulated by pinching off the tube and electron-beam-welding the pinch. The two samples from one laboratory were run only in the copper containers. The six samples from the other laboratory were run first in the copper containers and then repackaged in polyethylene vials after cutting off the ends of the potassium. The lower oxygen values for the polyethylene-contained samples are an indication that oxygen contamination of the copper can occur in the sealing procedure. All eight samples were analyzed using the same procedure as previously described. These data are listed in Table 11.

### SOURCES OF ERROR

In the determination of oxygen, using the fast-neutron-induced neutron-proton reaction, some of the principal nuclei of oxygen ( $O^{16}$ ) are converted to  $N^{16}$  nuclei. The unique properties of this radionuclide (short half-life and very high-energy beta particles and gamma rays) provide a relatively interference-free analytical procedure for the determination of oxygen. There are, however, certain matrix and geometry effects which can significantly affect the data. These problems are listed below, along with some of the techniques that have been used to reduce or correct for their effects.

#### Interelement Effect, $F^{19}(n,\alpha)N^{16}$

Fluorine is the only element, other than oxygen, that yields  $N^{16}$  when bombarded with fast neutrons. The cross section for this reaction is approximately 60% as great as that for the  $O^{16}(n,p)N^{16}$  reaction, with D-T neutrons. It is possible to determine the fluorine separately by measuring the 29.4-second  $O^{19}$  from the  $F^{19}(n,p)O^{19}$  reaction, or the 110-minute  $F^{18}$  from the  $F^{19}(n,2n)F^{18}$  reactions. Once the fluorine is known, its contribution to the total  $N^{16}$  can be subtracted and the oxygen obtained by difference. These techniques are effective for F:O ratios up to about 10. Above this level, the errors involved in subtracting one number from another that is only slightly larger render the technique useless.

#### Beta-Gamma Overlap

Because of the high energy of the  $N^{16}$   $\beta$ - $\gamma$  rays, interference in the oxygen procedure from matrix activities (other elements) is not as serious as in other elemental procedures. There are several common elements, however, which do yield fairly high-energy beta and/or gamma rays when

Table 11  
 DETERMINATION OF OXYGEN IN POTASSIUM SAMPLES  
 FROM NASA CONTRACTORS

Sample	Capsule Material	Weight (g)	Mg Oxygen				Average ppm O	
			1st	2nd	Average	Blank		Net
Laboratory A								
1	Polyethylene	1.6736	1.632	1.628	1.630	1.548	0.082	49
2	Polyethylene	1.3217	1.828	1.812	1.820	1.548	0.272	206
3	Polyethylene	2.2873	1.824	1.778	1.801	1.548	0.253	110
4	Polyethylene	1.4322	1.939	1.981	1.960	1.548	0.412	285
5	Polyethylene	1.2810	1.762	1.816	1.789	1.548	0.241	188
6	Polyethylene	1.3512	1.793	1.835	1.814	1.548	0.266	197
1	Copper	2.2678	0.786	0.752	0.769	0.675	0.094	42
2	Copper	2.6067	1.240	1.233	1.237	0.675	0.562	216
3	Copper	1.4530	0.822	0.868	0.845	0.675	0.170	117
4	Copper	0.6549	0.973	1.012	0.993	0.675	0.318	485
5	Copper	1.5822	1.132	1.155	1.144	0.675	0.469	296
6	Copper	1.6602	1.019	1.089	1.054	0.675	0.379	228
Laboratory B								
1	Copper	2.3899	0.743	0.766	0.755	0.684	0.071	30
2-1	Copper	2.0948	1.218	1.188	1.203	0.684	0.519	247
2-2	Copper	2.4006	1.261	1.234	1.248	0.684	0.564	243

irradiated with fast neutrons, and it is essential that the proper electronic discrimination be maintained for good results. Some of the common elements which must be considered are listed in Table 12.

Table 12  
PRODUCTS OF THE FAST-NEUTRON IRRADIATION OF SOME COMMON  
MATRIX AND IMPURITY ELEMENTS

Element	Reaction	Product Half-life	Product Energy (Mev)	
			Gamma	Beta
Lithium	$\text{Li}^7(\text{n}, \alpha)\text{H}^3$	12.3 yr	-----	0.018
	$\text{Li}^6(\text{n}, \alpha)\text{H}^3$	12.3 yr	-----	0.018
Sodium	$\text{Na}^{23}(\text{n}, \alpha)\text{F}^{20}$	10.7 sec	1.63	5.4
	$\text{Na}^{23}(\text{n}, \text{p})\text{Ne}^{23}$	40 sec	0.44	4.4, 4.0
Potassium	$\text{K}^{39}(\text{n}, 2\text{n})\text{K}^{38}$	7.7 min	2.16	2.68( $\beta^+$ )
	$\text{K}^{41}(\text{n}, \text{p})\text{Ar}^{41}$	110 min	1.29	1.20
	$\text{K}^{41}(\text{n}, \alpha)\text{Ca}^{38}$	37.3 min	2.16, 1.59	4.8, 2.8, 1.1
Rubidium	$\text{Rb}^{87}(\text{n}, \text{p})\text{Kr}^{87}$	78 min	2.57, 0.403	3.8, 1.3
	$\text{Rb}^{87}(\text{n}, \alpha)\text{Br}^{84}$	6.0 min	1.46, 0.88, 0.44	1.9, 0.8
	$\text{Rb}^{85}(\text{n}, 2\text{n})\text{Rb}^{84\text{m}}$	23 min	0.463, 0.239	-----
Cesium	$\text{Cs}^{133}(\text{n}, \alpha)\text{I}^{130}$	12.6 hr	1.15, 0.744, 0.660, 0.528, 0.409	1.02, 0.60
Fluorine	$\text{F}^{19}(\text{n}, \alpha)\text{N}^{16}$	7.35 sec	7.1, 6.1	10.4, 4.3, 3.3
	$\text{F}^{19}(\text{n}, \text{p})\text{O}^{19}$	29.4 sec	1.4, 0.2	4.5, 2.9
Sulfur	$\text{S}^{34}(\text{n}, \text{p})\text{P}^{34}$	12.4 sec	2.1	5.1, 3.2
Chlorine	$\text{Cl}^{37}(\text{n}, \text{p})\text{S}^{37}$	5.0 min	3.1	4.3, 1.6
	$\text{Cl}^{37}(\text{n}, \alpha)\text{P}^{34}$	12.4 sec	2.1	5.1, 3.2
Magnesium	$\text{Mg}^{26}(\text{n}, \alpha)\text{Ne}^{23}$	40 sec	0.44	4.4, 4.0
	$\text{Mg}^{24}(\text{n}, \text{p})\text{Na}^{24}$	14.9 hr	2.75, 1.37	1.4
Boron	$\text{B}^{11}(\text{n}, \text{p})\text{Be}^{11}$	14.1 sec	6.8(?), 2.1	11.5, 9.4
	$\text{B}^{11}(\text{n}, \alpha)\text{Li}^8$	0.9 sec	-----	13, 6, 3

The magnitude of interference from these elements is easily seen by irradiating each one individually with the same neutron flux needed to produce 1000 counts from 100 ppm of oxygen. The concentration of each element needed to produce the same 1000 counts can be plotted as a function of the discriminator setting (Mev). A summary of this experiment is given in Table 13, which includes many of the elements cited in Table 12. Since the boron activity is largely beta, it can be removed with lead absorbers.

Table 13

CONCENTRATION OF ELEMENT REQUIRED TO GIVE SAME  
COUNT AS 100 ppm OXYGEN

Discriminator Setting (Mev)	Element (ppm)					
	F	B	Na	S	Cl	Mg
1.5	130	385	120	12,700	5,000	6,600
2.5	170	435	7,200	----	24,000	16,000
3.5	170	495	---	----	----	25,000
4.5	170	610	---	----	----	----

Recoil Interference

Irradiation of samples in the presence of oxygen gas can lead to high values due to a recoil mechanism. The resulting  $N^{16}$  formed near the sample is trapped on the surface by absorption and/or chemical bonding and returns with the sample to the detectors. The effect is much more serious with metal samples, particularly copper, than with organic polymers. The magnitude of this problem is shown in Table 14. In this case, the samples of copper and polyethylene were irradiated separately and together, in air and in nitrogen. The increase in apparent oxygen for the polyethylene with the air irradiation (0.9 mg O) represents a serious problem, but it is five times smaller than the effect with copper. A possible explanation for this difference is the electron availability of the copper versus the polymer. This problem can be eliminated, however, by the use of nitrogen in the transfer system.

Table 14

RESULTS OF IRRADIATION IN PRESENCE  
OF OXYGEN GAS

Sample	Environment	Oxygen Found (mg)
Copper	Air	6.8
Copper	Nitrogen	2.0
Polyvial	Air	2.2
Polyvial	Nitrogen	1.3
Cu inside polyvial	Air	4.3
Cu inside polyvial	Nitrogen	3.4

### Beta-Gamma Attenuation

In the measurement of  $N^{16}$  for oxygen determinations, both gamma rays and beta particles may contribute to the observed activity. Since this activity originates inside the sample, it is subject to attenuation. Failure to account for the differences in sample density can lead to serious errors, particularly in the lower Z elements. In one series of experiments, metals of varying densities were drilled and fitted with a small Lucite rod in the center. Each metal, then, had essentially the same amount of oxygen in the center, and all were given identical irradiations. The only variable in the measured activity was the attenuation in the metal matrix. The results of this experiment are summarized in Table 15.

Table 15  
BETA-GAMMA ATTENUATION

Sample	Areal Density (g/cm <sup>2</sup> )	Relative Count Rate (%)
Be	0.6	140
Al	1.2	120
Ti	1.7	112
Ce	2.4	102
Fe	3.0	100
Pb	3.6	95

### Pulse Pileup

Pulse pileup results from a matrix that has a high cross section for fast neutrons, leading to large amounts of activity. If more than one gamma-ray photon strikes the NaI(Tl) crystal within the resolving time of the detection system, the energy is summed and counted as a single gamma-ray interaction. For example, if two 0.51-Mev gamma rays enter the system at nearly the same time, the result appears as a pulse of 1.02 Mev. In a case where the discriminator is set at 5 Mev, it would require 10 simultaneous 0.51-Mev gamma rays to result as a count. This type of activity ( $\sim 200$  mr/hr) is within the capability of an accelerator producing  $10^9$  n/cm<sup>2</sup>-sec. Some of the materials that can produce this effect are Ba, Al, Sb, Cu, Rb, Si, Sr, V, and Zr. Since most of the elements produce long-lived activities (half-lives of minutes or hours) the pileup is not serious in the first oxygen determination. It is usually only after several determinations with the same sample that the activity level becomes a problem.

Flux Gradient

The neutron flux varies with distance from a point source as  $1/r^2$ , where  $r$  is the distance between the neutron source and the sample. For a disk source (which is more nearly the case with the Cockroft-Walton target), the situation is more involved, but the decrease of neutron flux with distance is still large. In practice, this means that there will be a difference in activity in a cylinder 1/2 inch in diameter and 1-1/2 inches long (capsule size) from one side to the other. When such a sample is counted between two 3-inch by 3-inch NaI(Tl) detectors, an error of up to 5% is possible. This error can be eliminated by rotating the sample during the irradiation step. Table 16 shows the increase in precision available by rotating the sample and the monitor at 94 rpm in the neutron field.

Table 16  
EFFECT OF SAMPLE ROTATION DURING  
NEUTRON IRRADIATION

Oxygen Added (mg)	Sample Count	Monitor Count	Oxygen Found (mg)	% Error
Rotation of Sample and Monitor <sup>a</sup>				
69.1	23,511	13,220	67.4	2.5
69.1	23,820	12,820	69.4	0.3
69.1	23,760	12,690	70.1	1.4
69.1	23.213	12,730	68.9	0.3
69.1	20.940	11,260	70.5	<u>2.0</u>
				1.3 avg
No Rotation				
69.1	19,940	11,880	63.6	8.0
69.1	22,730	11,590	74.6	8.0
69.1	23,640	12,260	69.8	1.0
69.1	23,870	13,060	66.5	3.8
69.1	21.860	11,590	71.4	<u>3.3</u>
				4.8 avg

<sup>a</sup> Sample contained 69.1 mg oxygen as oxalic acid sealed in polyethylene. Monitor was 1/2-in. -diam by 2-in. -long Lucite rod. Both rotated during irradiation.

## VI. SUMMARY AND CONCLUSIONS

The development of neutron activation analysis procedures for the determination of oxygen in potassium under the NASA Lewis Research Center Contract NAS3-2537 has produced an analytical system that is representative of the best state of the art at the present time. The significance of the improvements that evolved during the course of the investigation can be seen in the improved sensitivity, precision, accuracy, speed of analysis, reliability, and ease of operation of the equipment now available. The oxygen sensitivity of detection, for example, at the beginning of the contract period was approximately 200 photopeak counts per milligram of oxygen. At the present time, the sensitivity is a factor of ten greater than this. A new model of the accelerator accounted for a factor of three improvement, and the remainder was the result of faster transfer times, better irradiation geometry, improved detector arrangement, and faster electronics. This same factor of ten applies to the lower limit of detection, which has dropped from 250  $\mu\text{g}$  to 25  $\mu\text{g}$  during the course of this contract. Without these improvements, none of the potassium samples submitted by NASA-Lewis could have been accurately analyzed.

The precision and accuracy of the method have also been greatly improved. Prior to this investigation, one standard deviation for a series of oxygen determinations on any type sample was between  $\pm 4\%$  and  $\pm 10\%$  for high oxygen levels (0.1% to 10% oxygen) and  $\pm 40\%$  at the lower limit of 250  $\mu\text{g}$  O. The present system will produce precisions of  $\pm 1\%$  at the higher oxygen levels and very near the theoretical value (based on just the counting statistics) at the lower limit of 25  $\mu\text{g}$  ( $\pm 26\%$  versus  $\pm 24\%$  theoretical). The dual transfer system, which essentially eliminates timing and neutron production monitoring errors, the automatic control unit, which eliminates operator errors, and the spinning terminal end, which averages the non-uniform flux gradient, have all contributed to the increased precision and accuracy. A better understanding of the other sources of error, such as recoil, pulse pileup, and electronic discrimination, have also helped in this respect.

Increases in the speed, reliability, and ease of operation of the system are a direct result of automating the procedures.

The procedures for handling potassium prior to analysis have also been improved. The development of encapsulation techniques using specially cleaned copper has made it possible to analyze for oxygen even

in the 25- to 35- $\mu\text{g}$  range. By allowing the 9.7-minute  $\text{Cu}^{62}$  to decay between determinations, the samples can be rerun as often as desired. Stainless-steel capsules have better structural and nuclear properties, but low-oxygen-content steels are not yet available in commercial quantities. Republic Steel Corporation is producing a variety of steels on a pilot-plant scale; these are quite acceptable, but it will be four or five months before they will be available for use in routine analysis.

Based on General Atomic's experience with a number of laboratories, it appears that a repackaging procedure may be necessary for alkali metals. In this case, an analytical sample is taken from the matrix of the material, thus eliminating any surface contamination which may have occurred when the original sample was taken. Any contamination in the highly monitored inert atmosphere could be standardized and a correction applied to the final results.

The principal conclusions to be drawn from this investigation are the following:

1. Oxygen concentrations can be sensitively, precisely, accurately, rapidly, and nondestructively determined in a potassium matrix by activation analysis methods.
2. The practical defined lower limit of detection is now 25  $\mu\text{g}$  of oxygen for a single determination.
3. The practical maximum sample volume is about 8 cubic centimeters.
4. An 8-cubic-centimeter-sample volume will hold approximately 7 grams of potassium. At the 25- $\mu\text{g}$ -oxygen level, this corresponds to an oxygen concentration of 3.5 ppm.
5. At the 1-ppm-oxygen level, the uncertainty would be  $\pm 0.7$  ppm for a single determination. This uncertainty can be reduced by redetermining the sample several times.
6. The best presently available capsule material for low-oxygen-content potassium samples is OFHC copper.
7. An automated activation analysis system eliminates the need for a highly trained analyst.
8. The most sensitive detection system for  $\text{N}^{16}$  at the present time is one employing two large NaI(Tl) crystals.



9. Use of a single-channel pulse-height analyzer eliminates the need for a printout device and spectrum summing. This reduces the analytical time by 50%.
10. Nuclear reactors produce ample fast-neutron fluxes for oxygen determinations, but they induce too much activity in the capsules and in the potassium for practical application at this time.
11. For those interested in utilizing the technique now or in the near future, two possibilities exist: (1) having samples analyzed by this method through an existing commercial service, or (2) constructing a system in their own laboratories. Both possibilities are currently available and reasonable in cost. It should be emphasized, however, that precise determinations of oxygen in the alkali metals are dependent upon proper handling of the sample and capsule. In general, this means an elaborate inert atmosphere or vacuum system along with special cleaning apparatus for the capsule. The time involved and consequently the cost of analyzing these types of samples are greater than for oxygen-insensitive materials.

## VII. FUTURE WORK

On the basis of the findings of this investigation, there are two areas in which the desirability of further work is strongly indicated. First, the capsule material should be improved. Although it is possible to obtain copper containing as little as 2 ppm O, it is difficult to design a structurally sound capsule weighing less than 20 grams. This produces a blank of 40  $\mu\text{g}$  O. Copper also becomes very radioactive ( $\text{C}^{62}$ ) after several 20-second irradiations, and pulse pileup then becomes serious. A solution to this problem may be the use of research-grade steel now being produced by several large steel companies. These metals are being produced as part of the study of the new vacuum-furnace techniques. Several grades of stainless steel from these programs contain approximately 4 ppm O. Since a strong capsule can be constructed from even 5 grams of steel, this would immediately lower our blank by a factor of 2. Another potential source of good capsule material would be one of the newer polyolefins. General Atomic is currently trying to locate an acceptable grade of polypropylene. A California plastic-molding company has agreed to mold the capsules if a suitable polymer can be located. Polypropylene should also be less permeable to gaseous oxygen than polyethylene.

The second area in which a sizable gain can be made is that of sensitivity. The efficiency of the 3-inch by 3-inch NaI(Tl) detector is lower for the 6.13 - to 7.13-Mev gamma rays from  $\text{N}^{16}$  than that of a 5-inch by 5-inch NaI(Tl) detector. An order for a larger crystal was placed 9 months ago but delivery was too late for it to be used to obtain data for this report. Preliminary indications are, however, that it is better by a factor of 3 than the 3-inch by 3-inch crystal now in use. Thus the defined lower limit of detection may become only 8  $\mu\text{g}$   $\text{O}_3$  with an uncertainty of  $\pm 1.9 \mu\text{g}$ . With an optimum sample size (8  $\text{cm}^3$ ), this corresponds to a concentration of approximately 1 ppm of oxygen, determinable to  $\pm 0.25$  ppm.

VIII. REPORTABLE ITEMS OF NEW TECHNOLOGY  
DURING REPORT PERIOD

None.

REFERENCES

1. Elbling, P., and G. W. Goward, Anal. Chem. 32, 1610 (1960).
2. Griffiths, V. S., and M. I. Jackman, Anal. Chem. 31, 161 (1959).
3. Harris, W. F., and W. M. Hickam, Anal. Chem. 31, 1115 (1959).
4. Kallmann, S., and F. Collier, Anal. Chem. 32, 1617 (1960).
5. Coleman, R. F., and J. L. Perkin, Analyst 84, 233 (1959).
6. Fogelstrom-Fineman, I., et al., Intern. J. Appl. Radiation and Isotopes 2, 280 (1957).
7. Sue, P., Compt. Rend. 242, 770 (1956).
8. Osmund, R. G., and A. A. Smales, Anal. Chim. Acta 10, 117 (1954).
9. Lévêque, P., "Examples of Activation Analysis," First Geneva Conference Proceedings, United Nations, Geneva, 1955, v. 15, p. 78-80 (P/342).
10. Faull, N., "An Experimental Study of Neutron Induced Activities in Water," U.K. Atomic Energy Research Establishment Report AERE-R/R-1919, 1957.
11. Ajzenberg, F., and T. Lauritsen, Rev. Mod. Phys. 27, 77 (1955).
12. Veal, D. J., and C. F. Cook, Anal. Chem. 34, 178 (1962).
13. Steele, E. L., and W. W. Meinke, Anal. Chem. 34, 185 (1962).
14. Fujii, I., et al., Japan Analyst (in press).

## DL-1

## DISTRIBUTION LIST

National Aeronautics and Space Administration Washington 25, D. C. Attn: Walter C. Scott	1	National Aeronautics and Space Administration Lewis Research Center 21000 Brookpark Road Cleveland, Ohio 44135 Attn: R. A. Lindberg MS 500-309	4
National Aeronautics and Space Administration Washington 25, D. C. Attn: James J. Lynch	1	National Aeronautics and Space Administration Lewis Research Center 21000 Brookpark Road Cleveland, Ohio 44135 Attn: Normal T. Musial, Patent Counsel MS 77-1	1
National Aeronautics and Space Administration Scientific & Technical Information Facility Box 5700 Bethesda 14, Maryland Attn: NASA Representative	2+ repro	National Aeronautics and Space Administration Lewis Research Center 21000 Brookpark Road Cleveland, Ohio 44135 Attn: T. A. Moss MS 500-309	1
National Aeronautics and Space Administration Washington 25, D. C. Attn: George C. Deutsch (RR)	1	National Aeronautics and Space Administration Lewis Research Center 21000 Brookpark Road Cleveland, Ohio 44135 Attn: Dr. Louis Rosenblum (MSD) MS 106-1	1
National Aeronautics and Space Administration Ames Research Center Moffet Field, California Attn: Librarian	1	National Aeronautics and Space Administration Lewis Research Center 21000 Brookpark Road Cleveland, Ohio 44135 Attn: Glenn R. Zellars MS 106-1	1
National Aeronautics and Space Administration Goddard Space Flight Center Greenbelt, Maryland Attn: Librarian	1	National Aeronautics and Space Administration Lewis Research Center 21000 Brookpark Road Cleveland, Ohio 44135 Attn: Judson Graab MS 105-1	1
National Aeronautics and Space Administration Langley Research Center Hampton, Virginia Attn: Librarian	1	National Aeronautics and Space Administration Lewis Research Center 21000 Brookpark Road Cleveland, Ohio 44135 Attn: John E. Dilley MS 500-309	1
National Aeronautics and Space Administration Lewis Research Center 21000 Brookpark Road Cleveland, Ohio 44135 Attn: Librarian	1	National Aeronautics and Space Administration Lewis Research Center 21000 Brookpark Road Cleveland, Ohio 44135 Attn: Office of Reliability and Quality Assurance	1
National Aeronautics and Space Administration Lewis Research Center 21000 Brookpark Road Cleveland, Ohio 44135 Attn: Dr. Bernard Lubarsky (SPSD) MS 500-201	1	National Aeronautics and Space Administration Manned Spacecraft Center Houston 1, Texas Attn: Librarian	1
National Aeronautics and Space Administration Lewis Research Center 21000 Brookpark Road Cleveland, Ohio 44135 Attn: Roger Mather (SEPO) MS 500-309	1		
National Aeronautics and Space Administration Lewis Research Center 21000 Brookpark Road Cleveland, Ohio 44135 Attn: G. M. Ault MS 105-1	1		

DI.-2

National Aeronautics and Space Administration George C. Marshall Space Flight Center Huntsville, Alabama Attn: Librarian	1	U. S. Atomic Energy Commission Germantown, Maryland Attn: Col. E. L. Douthett	1
National Aeronautics and Space Administration Jet Propulsion Laboratory 4800 Oak Grove Drive Pasadena 3, California Attn: Librarian	1	U. S. Atomic Energy Commission Germantown, Maryland Attn: H. Rothen	1
National Aeronautics and Space Administration Western Operations Office 150 Pico Boulevard Santa Monica, California Attn: John Keeler	1	U. S. Atomic Energy Commission Germantown, Maryland Attn: Major Gordon Dicker	1
National Aeronautics and Space Administration Western Operations Office 150 Pico Boulevard Santa Monica, California Attn: Leon Dondi	1	U. S. Atomic Energy Commission Germantown, Maryland Attn: Socrates Christofer	1
National Bureau of Standards Washington 25, D. C. Attn: Librarian	1	U. S. Atomic Energy Commission Technical Information Service Extension P. O. Box 62 Oak Ridge, Tennessee	3
Aeronautical Systems Division Wright-Patterson Air Force Base, Ohio Attn: Charles Armbruster ASRPP-10	1	U. S. Atomic Energy Commission Washington 25, D. C. Attn: M. J. Whitman	1
Aeronautical Systems Division Wright-Patterson Air Force Base, Ohio Attn: T. Cooper	1	Argonne National Laboratory 9700 South Cass Avenue Argonne, Illinois 60440 Attn: Librarian	1
Aeronautical Systems Division Wright-Patterson Air Force Base, Ohio Attn: Librarian	1	Brookhaven National Laboratory Upton, Long Island, New York 11973 Attn: Librarian	1
Aeronautical Systems Division Wright-Patterson Air Force Base, Ohio Attn: George M. Glenn	1	Oak Ridge National Laboratory Oak Ridge, Tennessee Attn: W. C. Thurber	1
Army Ordnance Frankford Arsenal Bridesburg Station Philadelphia 37, Pennsylvania Attn: Librarian	1	Oak Ridge National Laboratory Oak Ridge, Tennessee Attn: Dr. A. J. Miller	1
Bureau of Mines Albany, Oregon Attn: Librarian	1	Oak Ridge National Laboratory Oak Ridge, Tennessee Attn: Librarian	1
Bureau of Ships Department of the Navy Washington 25, D. C. Attn: Librarian	1	Office of Naval Research Power Division Washington 25, D. C. Attn: Librarian	1
U. S. Atomic Energy Commission Headquarters Library Reports Section Mail Station G-017 Washington, D. C. 20545	1	U. S. Naval Research Laboratory Washington 25, D. C. Attn: Librarian	1
U. S. Atomic Energy Commission P. O. Box 1102 Middletown, Connecticut Attn: C. E. McColley CANEL Project Office	1	Advanced Technology Laboratories Division of American Standard 369 Whisman Road Mountain View, California Attn: Librarian	1

## DL-3

Aerojet General Corporation P. O. Box 296 Azusa, California Attn: Librarian	1	The Boeing Company Seattle, Washington Attn: Librarian	1
Aerojet General Nucleonics P. O. Box 78 San Ramon, California Attn: Librarian	1	Brush Beryllium Company Cleveland, Ohio Attn: Librarian	1
AiResearch Manufacturing Company Sky Harbor Airport 402 South 36th Street, Phoenix, Arizona Attn: Librarian	1	Carborundum Company Niagara Falls, New York Attn: Librarian	1
AiResearch Manufacturing Company Sky Harbor Airport 402 South 36th Street, Phoenix, Arizona Attn: E. A. Kovacivich	1	Chance Vought Corporation P. O. Box 3907 Dallas 22, Texas Attn: Librarian	1
AiResearch Manufacturing Company 9851-9951 Sepulveda Boulevard Los Angeles 45, California Attn: Librarian	1	Climax Molybdenum Company of Michigan Detroit, Michigan Attn: Librarian	1
Allis Chalmers Atomic Energy Division Milwaukee, Wisconsin Attn: Librarian	1	General Dynamics/Astronautics 5001 Kearny Villa Road San Diego 11, California Attn: Librarian	1
Allison General Motors Energy Conversion Division Indianapolis, Indiana Attn: Librarian	1	Crucible Steel Company of America Pittsburgh, Pennsylvania Attn: Librarian	1
AMF Atomics 140 Greenwich Avenue Greenwich, Connecticut Attn: Librarian	1	Curtiss-Wright Corporation Research Division Tuehanna, Pennsylvania Attn: Librarian	1
Armour Research Foundation 10 W. 35th Street Chicago 16, Illinois Attn: Librarian	1	Dartmouth College Hanover, New Hampshire Attn: Librarian	1
Avco Research and Advanced Development Dept. 201 Lowell Street Wilmington, Massachusetts	1	E. I. duPont de Nemours & Company, Inc. Wilmington 93, Delaware Attn: Librarian	1
Babcock and Wilcox Company Research Center Alliance, Ohio Attn: Librarian	1	Edgerton, Germeshausen & Grier, Inc. Santa Barbara Airport Goleta, California Attn: Librarian	1
Battelle Memorial Institute 505 King Avenue Columbus, Ohio Attn: Librarian	1	Electro-Optical Systems, Incorporated Advanced Power Systems Division Pasadena, California Attn: Librarian	1
The Bendix Corporation Research Laboratories Division Southfield, Detroit 1, Michigan Attn: Librarian	1	Fansteel Metallurgical Corporation North Chicago, Illinois Attn: Librarian	1
		Firth Sterling, Incorporated McKeesport, Pennsylvania Attn: Librarian	1
		Ford Motor Company Aeronutronics Newport Beach, California Attn: Librarian	1

## DL-4

General Electric Company Atomic Power Equipment Division P.O. Box 1131 San Jose, California	1	Los Alamos Scientific Laboratory University of California Los Alamos, New Mexico Attn: Librarian	1
General Electric Company Missile & Space Vehicle Department 3198 Chestnut Street Philadelphia 4, Pennsylvania Attn: Librarian	1	ManLabs, Incorporated 21 Erie Street Cambridge 39, Massachusetts Attn: Librarian	1
General Electric Company Vallecitos Atomic Laboratory Pleasanton, California Attn: Librarian	1	Marquardt Aircraft Company P.O. Box 2013 Van Nuys, California Attn: Librarian	1
General Dynamics/Fort Worth P.O. Box 748 Fort Worth, Texas Attn: Librarian	1	The Martin Company Baltimore 3, Maryland Attn: Librarian	1
General Motors Corporation Allison Division Indianapolis 6, Indiana Attn: Librarian	1	The Martin Company Nuclear Division P.O. Box 5042 Baltimore 20, Maryland Attn: Librarian	1
Hamilton Standard Division of United Aircraft Corporation Windsor Locks, Connecticut Attn: Librarian	1	Martin Marietta Corporation Metals Technology Laboratory Wheeling, Illinois	1
High Voltage Engineering Corporation Burlington, Massachusetts Attn: Librarian	1	Massachusetts Institute of Technology Cambridge 39, Massachusetts Attn: Librarian	1
Hughes Aircraft Company Engineering Division Culver City, California Attn: Librarian	1	Materials Research Corporation Orangeburg, New York Attn: Librarian	1
Kaman Nuclear Division Kaman Aircraft Corporation Colorado Springs, Colorado Attn: Librarian	1	McDonnell Aircraft St. Louis, Missouri Attn: Librarian	1
Kennametal, Incorporated Latrobe, Pennsylvania Attn: Librarian	1	Michigan State University East Lansing, Michigan Attn: Librarian	1
Kodak Research Labs 343 State Street Rochester, New York Attn: Librarian	1	MSA Research Corporation Callery, Pennsylvania Attn: Librarian	1
Kodak Research Labs 343 State Street Rochester, New York Attn: Librarian	1	National Research Corporation 405 Industrial Place Newton, Massachusetts Attn: Librarian	1
Latrobe Steel Company Latrobe Pennsylvania Attn: Librarian	1	New Hampshire University Durham, New Hampshire Attn: Librarian	1
Lockheed Georgia Company Division of Lockheed Aircraft Company Marietta, Georgia Attn: Librarian	1	New Mexico University Albuquerque, New Mexico Attn: Librarian	1
Lockheed Missiles and Space Division Lockheed Aircraft Corporation Sunnyvale, California Attn: Librarian	1	North American Aviation Los Angeles Division Los Angeles 9, California Attn: Librarian	1



## DL-5

Norton Company Worcester, Massachusetts Attn: Librarian	1	Union Carbide Metals Niagara Falls, New York Attn: Librarian	1
Pennsylvania University 3440 Woodland Avenue Philadelphia, Pennsylvania Attn: Librarian	1	United Nuclear Corporation Five New Street White Plains, New York Attn: Librarian	1
Pratt & Whitney Aircraft 400 Main Street East Hartford 8, Connecticut Attn: Librarian	1	University of Michigan Department of Chemical and Metallurgical Engineering Ann Arbor, Michigan Attn: Librarian	1
Republic Aviation Corporation Farmingdale, Long Island, New York Attn: Librarian	1	Wah Chang Corporation Albany, Oregon Attn: Librarian	1
Rocketdyne Canoga Park, California Attn: Librarian	1	Westinghouse Electric Corporation Astronuclear Laboratory P. O. Box 10864 Pittsburgh 36, Pennsylvania Attn: Librarian	1
Solar 2200 Pacific Highway San Diego 12, California Attn: Librarian	1	Westinghouse Electric Corporation Astronuclear Laboratory P. O. Box 10864 Pittsburgh 36, Pennsylvania Attn: R. T. Begley	1
Southern Regional Research Laboratory New Orleans, Louisiana Attn: Librarian	1	Wolverine Tube Division Calumet & Hecla, Inc. 17200 Southfield Road Allen Park, Michigan Attn: Mr. Eugene F. Hill	1
Southwest Research Institute 8500 Culebra Road San Antonio 6, Texas Attn: Librarian	1	Ilikon Corporation Natick Industrial Center Natick, Massachusetts Attn: Librarian	1
Stanford Research Institute Menlo Park, California Attn: Librarian	1	Ilikon Corporation Natick Industrial Center Natick, Massachusetts Attn: Dr. Seige Matsoda	1
Superior Tube Company Morristown, Pennsylvania Attn: Mr. A. Bound	1	American Machine and Foundry Company Alexandria Division 1023 Worth Royal Street Alexandria, Virginia Attn: Librarian	1
Sylvania Electrics Products, Inc. Chemical and Metallurgical Towanda, Pennsylvania Attn: Librarian	1	Douglas Aircraft Company, Inc. Missile and Space Systems Division 300 Ocean Park Boulevard Santa Monica, California Attn: Library	1
Thompson Ramo Wooldridge, Inc. Caldwell Research Center 23555 Euclid Avenue Cleveland 17, Ohio Attn: Librarian	1	Nuclide Analysis Associates P. O. Box 752 State College, Pennsylvania	1
Thompson Ramo Wooldridge, Inc. Caldwell Research Center 23555 Euclid Avenue Cleveland 17, Ohio Attn: G. J. Guarnieri	1		
Thompson Ramo Wooldridge, Inc. New Devices Laboratories 7209 Platt Avenue Cleveland 4, Ohio Attn: Librarian	1		

## DL-6

General Electric Company Chemical and Materials Engineering Laboratory Advanced Technology Laboratories Schenectady, New York Attn: Librarian	1	Westinghouse Research Laboratories Pittsburgh 35, Pennsylvania Attn: Librarian	1
Lessona Moes Laboratories Lake Success Park, Community Drive Great Neck, Long Island, New York Attn: Librarian	1	Bureau of Weapons Research and Engineering Material Division Washington 25, D. C. Attn: Librarian	1
Nuclear Metals, Inc. West Concord, Massachusetts Attn: Librarian	1	E. I. du Pont de Nemours & Company, Inc. Wilmington 93, Delaware Attn: E. M. Hahla	1
North American Aviation, Inc. Atomic International Division P. O. Box 309 Canoga Park, California Attn: Librarian	1	Pratt & Whitney Aircraft CANEL P. O. Box 611 Middletown, Connecticut Attn: Librarian	2
North American Aviation, Inc. Atomics International Division P. O. Box 309 Canoga Park, California Attn: Dr. R. L. McKisson	2	General Electric Company Missiles and Space Division Cincinnati, Ohio 45215 Attn: Dr. J. W. Semmel	2
Westinghouse Electric Corporation Aerospace Electric Division Lima, Ohio Attn: Librarian	1	The Ledoux Company 359 Alfred Avenue Teaneck, New Jersey Attn: Mr. Silve Kallman	1